Inorganic Chemistry

Article

pubs.acs.org/IC

A Series of $M^{II}Cu^{II}_3$ Stars (M = Mn, Ni, Cu, Zn) Exhibiting Unusual Magnetic Properties

Suraj Mondal,[†] Shuvankar Mandal,[†] Luca Carrella,[‡] Arpita Jana,[†] Michel Fleck,[§] Andreas Köhn,[⊥] Eva Rentschler,*[,‡] and Sasankasekhar Mohanta*[,†]

[†]Department of Chemistry, University of Calcutta, 92 A. P. C. Road, Kolkata 700 009, India

[‡]Institut für Anorganische Chemie und Analytische Chemie, Johannes-Gutenberg Universität Mainz, Duesbergweg 10−14, D-55128 Mainz, Germany

[§]Institute for Mineralogy and Crystallography, University of Vienna, Althanstrasse 14, A-1090 Vienna, Austria

[⊥]Institut für Theoretische Chemie, Universität Stuttgart, Pfaffenwaldring 55, D-70569 Stuttgart, Germany

Supporting Information

ABSTRACT: The work in this report describes the syntheses, electrospray ionization mass spectromtery, structures, and experimental and density functional theoretical (DFT) magnetic properties of four tetrametallic stars of composition $[M^{II}(Cu^{II}L)_3](ClO_4)_2$ (**1**, M = Mn; **2**, M = Ni; **3**, M = Cu; **4**, M = Zn) derived from a single-compartment Schiff base ligand, *N*,*N*′-bis(salicylidene)-1,4-butanediamine (H_2L), which is the [2 + 1] condensation product of salicylaldehyde and 1,4-diaminobutane. The central metal ion (Mn^{II}, Ni^{II}, Cu^{II}, or Zn^{II}) is linked with two μ_2-phenoxo bridges of each of the three $[Cu^{II}L]$ moieties, and thus the central metal ion is encapsulated in between three $[Cu^{II}L]$ units. The title compounds are rare or sole examples of stars having these metal-ion combinations. In the cases of **1**, **3**, and **4**, the four metal ions form a centered isosceles triangle, while the four metal ions in **2** form a centered equilateral triangle. Both the variable-temperature magnetic susceptibility and variable-field magnetization (at 2−10 K) of **1**−**3** have been measured and simulated contemporaneously. While the $Mn^{II}Cu^{II}_3$ compound **1** exhibits ferromagnetic interaction with J = 1.02 cm^{-1}, the $Ni^{II}Cu^{II}_3$ compound **2** and $Cu^{II}Cu^{II}_3$ compound **3** exhibit antiferromagnetic interaction with J = −3.53 and −35.5 cm^{-1}, respectively. Variable-temperature magnetic susceptibility data of the $Zn^{II}Cu^{II}_3$ compound **4** indicate very weak antiferromagnetic interaction of −1.4 cm^{-1}, as expected. On the basis of known correlations, the magnetic properties of **1**−**3** are unusual; it seems that ferromagnetic interaction in **1** and weak/moderate antiferromagnetic interaction in **2** and **3** are possibly related to the distorted coordination environment of the peripheral copper(II) centers (intermediate between square-planar and tetrahedral). DFT calculations have been done to elucidate the magnetic properties. The DFT-computed J values are quantitatively (for **1**) or qualitatively (for **2** and **3**) matched well with the experimental values. Spin densities and magnetic orbitals (natural bond orbitals) correspond well with the trend of observed/computed magnetic exchange interactions.

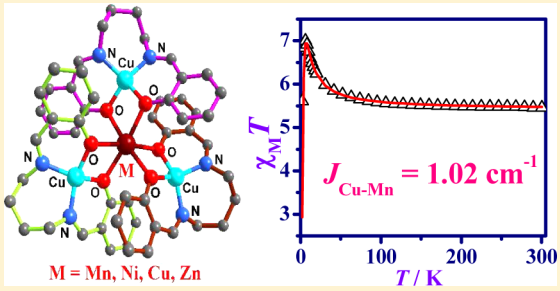

INTRODUCTION

Much development has been done in molecular magnetism over the decades starting from the 1950s.[1−14] It has been an interdisciplinary topic covering contributions from synthetic chemistry, materials science, and theoretical chemistry.[1−14] The intimate relationship of spin coupling has been understood from orbital models.[2] Utilization of density functional theory (DFT) in the modeling of magnetic phenomena has enriched the area tremendously.[9,13,14] Eventually, several experimental[2,8−14] and theoretical[8,13,14] magnetostructural correlations have been determined so that it is possible in several cases to predict or guess possible magnetic properties of new systems in terms of structural parameters and vice versa. However, in spite of the huge stock of reports of the magnetic properties of a variety of systems, studies of the magnetic properties of new types of exchange-coupled systems still deserve attention because of the possibility of the development of some unprecedented aspects.

Numerous metal compounds have been reported from the single-compartment (e.g., salicylaldehyde−diamine) or double-compartment (e.g., 3-methoxy/ethoxysalicylaldehyde−diamine) acyclic Schiff base ligands, obtained from the condensation of salicylaldehyde or 3-methoxy/ethoxysalicylaldehyde with diamines.[15−19] Metal complexes from such ligands were first reported in the 1960s[16] but are still being reported with interesting structures and properties.[15,17−19] Two ways for changing such ligands are (i) changing the substituent in the aldehyde component and (ii) changing the diamine component. It is worth mentioning that thousands of compounds

Received: August 4, 2014
Published: December 12, 2014

from this general class of ligands are known where the number of carbon atoms between the two imine nitrogen atoms is two or three.[15−19] On the other hand, metal complexes derived from such general ligands where there are four carbon atoms (i.e., the diamine component is 1,4-diaminobutane) are only a few.[15,18a,20,21] Therefore, with the expectation of getting interesting structures and accompanied properties, we have been motivated to explore the structures and properties of metal complexes derived from the above-mentioned types of ligands containing four carbon atoms between the two imine nitrogen atoms. Already, we have reported some compounds derived from *N*,*N*′-bis(salicylidene)-1,4-butanediamine (H_2L; Chart 1).[18a] Those compounds include one $Cd^{II}Cu^{II}_3$ star,

Chart 1. Chemical Structure of the Ligand H_2L

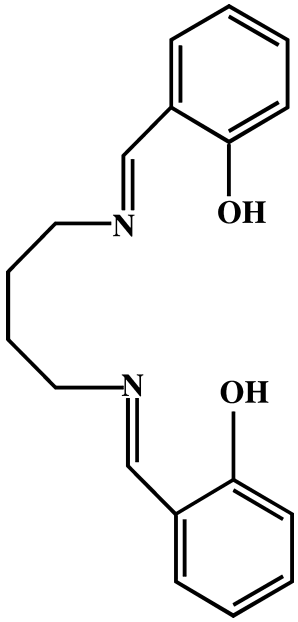

which is the best heterometallic star so far (in terms of the bond distances involving the central metal ion; all six Cd^{II}−phenoxo bond distances are equal). Therefore, we have been motivated to check the possibility of stabilization of such $M^{II}Cu^{II}_3$ stars, where M^{II} = late 3d metal ions. Because heterometallic stars are rare[15,18a,19b−d,22] and because $M^{II}Cu^{II}_3$ stars (where M^{II} = late 3d metal ions) are, in general, unprecedented, it would be interesting only in terms of the composition and structure. If such stars are stabilized, those would be interesting because it is nice for people to see the designed formation but not the accidental/unpredicted formation of the clusters. Moreover, the magnetic properties of such new types of systems would unveil some new aspects. With these aims, we proceeded and isolated four stars of composition $[M^{II}(Cu^{II}L)_3](ClO_4)_2$ (**1**, M = Mn; **2**, M = Ni; **3**, M = Cu; **4**, M = Zn). Herein, we report the syntheses, electrospray ionization mass spectromtery (ESI-MS), structures, and experimental and DFT magnetic properties of these compounds.

EXPERIMENTAL SECTION

Caution! *Perchlorate complexes of metal ions with organic ligands are potentially explosive. Only a small amount of material should be prepared, and it should be handled with care.*

Materials and Physical Measurements. All reagents and solvents were purchased from commercial sources and used as received. The mononuclear compound $[Cu^{II}L]$ was synthesized by the reported procedure.[18a] Elemental (C, H, and N) analyses were performed on a PerkinElmer 2400 II analyzer. IR spectra were recorded in the region 400−4000 cm^{-1} on a Bruker-Optics Alpha-T spectrophotometer with samples as KBr disks. Electronic spectra were obtained by using a Shimadzu UV-3600 spectrophotometer. The ESI-MS spectra were recorded on a Micromass Qtof YA 263 mass spectrometer. Magnetic measurements were carried out with a Quantum Design MPMS XL-7 SQUID magnetometer.

Syntheses of $[(Cu^{II}L)_3M^{II}](ClO_4)_2$ (1, M = Mn; 2, M = Ni; 3, M = Cu; 4, M = Zn). These four compounds were prepared following a general procedure as follows: An acetonitrile solution (5 mL) of the corresponding $M(ClO_4)_2·6H_2O$ (0.1 mmol) was dropwise added to a stirred suspension of $[Cu^{II}L]$ (0.108 g, 0.3 mmol) in acetonitrile (15 mL). After stirring for 30 min, the mixture was filtered and the filtrate (green for **1**, **2**, and **4**; reddish brown for **3**) was kept at room temperature for slow evaporation. After a few days, green crystalline compounds containing diffraction-quality crystals that deposited were collected by filtration, washed with cold acetonitrile, and dried in vacuo.

Data for ***1****.* Yield: 0.093 g (70%). Anal. Calcd for $C_{54}H_{54}N_6O_{14}Cl_2Cu_3Mn$: C, 48.86; H, 4.10; N, 6.33. Found: C, 48.57; H, 3.94; N, 6.50. Selected Fourier transform infrared (FT-IR) data on KBr (cm^{-1}): ν(C═N), 1629vs; $\nu(ClO_4)$, 1095vs and 623w.

Data for ***2****.* Yield: 0.107 g (80%). Anal. Calcd for $C_{54}H_{54}N_6O_{14}Cl_2Cu_3Ni$: C, 48.72; H, 4.09; N, 6.31. Found: C, 48.67; H, 4.21; N, 6.45. Selected FT-IR data on KBr (cm^{-1}): ν(C═N), 1626vs; $\nu(ClO_4)$, 1094vs and 622w.

Data for ***3****.* Yield: 0.098 g (73%). Anal. Calcd for $C_{54}H_{54}N_6O_{14}Cl_2Cu_4$: C, 48.54; H, 4.07; N, 6.29. Found: C, 48.42; H, 3.98; N, 6.41. Selected FT-IR data on KBr (cm^{-1}): ν(C═N), 1622vs; $\nu(ClO_4)$, 1094vs and 622w.

Data for ***4****.* Yield: 0.096 g (72%). Anal. Calcd for $C_{54}H_{54}N_6O_{14}Cl_2Cu_3Zn$: C, 48.48; H, 4.07; N, 6.28. Found: C, 48.62; H, 4.15; N, 6.09. Selected FT-IR data on KBr (cm^{-1}): ν(C═N), 1625vs; $\nu(ClO_4)$, 1094vs and 623w.

Structure Determination of 1−4. The crystallographic data for **1**−**4** are summarized in Table 1. X-ray diffraction data were collected on a Bruker-APEX II CCD diffractometer at 296 K using graphite-monochromated Mo Kα radiation (λ = 0.71073 Å). Because the crystals of all of the compounds **1**−**4** lose their crystalline nature as a result of removal of solvent molecules immediately after isolation, data of **1**−**4** were collected upon mounting of a crystal dipped in its mother liquor in a capillary. The data were processed using the packages *SAINT*.[23a] All data were corrected for Lorentz-polarization effects. Multiscan absorption corrections were made for all of the cases using the program *SADABS*.[23b] Structures were solved by direct and Fourier methods and refined by full-matrix least squares based on F^2 using *SHELXTL*[23c] and *SHELXL-97*[23d] packages.

During development of the structures, it was found that the following atoms were disordered over two positions: one carbon atom of the diamine moiety in each of **1** (C10) and **4** (C9); one perchlorate oxygen atom in each of **2** (O3) and **4** (O4); three perchlorate oxygen atoms (O4, O5, and O7) in **1**; four perchlorate oxygen atoms (O4, O5, O6, and O7) in **3**. The disorder was modeled by refining these two positions freely for each case and setting the sum of their occupancies to be equal to 1, and the final occupancy parameters were set as follows: 0.60/0.40 for C10A/C10B in **1** and O4A/O4B in **4**; 0.50/0.50 for C9A/C9B in **4**; 0.80/0.20 for O4A/O4B in **1**; 0.65/0.35 for O7A/O7B in **1**; 0.70/0.30 for O5A/O5B in **1**, O3A/O3B in **2**, and O4A/O4B, O5A/O5B, O6A/O6B, and O7A/O7B in **3**.

All hydrogen atoms were inserted at their geometrically calculated positions with isotropic thermal parameters and refined. All of the non-hydrogen atoms were refined anisotropically, while all of the hydrogen atoms were refined isotropically.

It was not possible to properly assign the solvent acetonitrile molecules in the structures of **1**, **3**, and **4**, and therefore these solvent molecules were eliminated by using the *SQUEEZE* facility of *PLATON* to improve the refinement.[23e] The electron counts per unit cell for the eliminated solvent molecules are 244, 160, and 168 for **1**, **3**, and **4**,

dx.doi.org/10.1021/ic501900d | *Inorg. Chem.* 2015, 54, 117−131

Table 1. Crystallographic Data for 1−4

	1 ($Mn^{II}Cu^{II}_3$)	2 ($Ni^{II}Cu^{II}_3$)	3 ($Cu^{II}Cu^{II}_3$)	4 ($Zn^{II}Cu^{II}_3$)
empirical formula	$C_{54}H_{54}N_6O_{14}Cl_2Cu_3Mn$	$C_{54}H_{54}N_6O_{14}Cl_2Cu_3Ni$	$C_{54}H_{54}N_6O_{14}Cl_2Cu_4$	$C_{54}H_{54}N_6O_{14}Cl_2Cu_3Zn$
fw	1327.49	1331.26	1336.09	1337.92
cryst syst	monoclinic	trigonal	monoclinic	monoclinic
space group	$I2/a$	$P\bar{3}c1$	$I2/a$	$I2/a$
a (Å)	26.4413(17)	14.547(7)	26.103(5)	26.137(2)
b (Å)	15.5908(9)	14.547(7)	15.193(2)	15.4273(11)
c (Å)	15.0859(9)	15.129(8)	15.384(3)	15.3494(11)
α (deg)	90.00	90.00	90.00	90.00
β (deg)	101.907(2)	90.00	100.822(5)	101.890(2)
γ (deg)	90.00	120.00	90.00	90.00
V (Å^3)	6085.2(6)	2773(2)	5992.5(18)	6056.5(8)
Z	4	2	4	4
T (K)	296(2)	296(2)	296(2)	296(2)
2θ	3.04−53.10	3.24−51.98	3.12−52.80	3.08−53.98
μ (mm^{-1})	1.390	1.637	1.556	1.584
ρ_{calcd} (g cm^{-3})	1.449	1.595	1.481	1.467
$F(000)$	2712	1362	2728	2732
abs corrn	multiscan	multiscan	multiscan	multiscan
index ranges	$-33 \le h \le 33$	$-17 \le h \le 17$	$-32 \le h \le 32$	$-32 \le h \le 32$
	$-17 \le k \le 18$	$-16 \le k \le 17$	$-17 \le k \le 18$	$-18 \le k \le 19$
	$-18 \le l \le 18$	$-18 \le l \le 17$	$-19 \le l \le 18$	$-19 \le l \le 19$
reflns collected	36756	18128	35120	35841
indep reflns (R_{int})	6217 (0.0613)	1816 (0.0391)	6069 (0.0433)	6482 (0.0589)
R1[a]/wR2[b] [$I > 2\sigma(I)$]	0.0609/0.1638	0.0437/0.1215	0.0445/0.1362	0.0505/0.1483
R1[a]/wR2[b] (for all F_o^2)	0.0862/0.1779	0.0662/0.1437	0.0610/0.1453	0.0854/0.1624

[a] $R1 = \sum||F_o| - |F_c||/\sum|F_o|$. [b] $wR2 = [\sum w(F_o^2 - F_c^2)^2/\sum w(F_o^2)^2]^{1/2}$.

respectively, indicating the presence of approximately 11 solvated acetonitrile molecules per unit cell in **1**, 7 or 8 solvated acetonitrile molecules per unit cell in **3**, and 8 solvated acetonitrile molecules per unit cell in **4**. Because the Z value for **1**, **3**, and **4** is 4, the numbers of solvated acetonitrile molecules per tetrametallic cluster in **1** and **3**/**4** are approximately three and two, respectively. However, as already mentioned, crystals of all of the compounds lose solvent molecules. In fact, elemental analyses and FT-IR spectra are well matched with a composition without any solvent molecule. Therefore, in the formulas of all of the compounds, solvent acetonitrile molecules are not considered.

The final refinement converged at the R1 [$I > 2\sigma(I)$] values of 0.0609, 0.0437, 0.0445, and 0.0505 for **1**−**4**, respectively.

Computational Details. Quantum chemical calculations were carried out with the *TURBOMOLE* program package, version 6.5 and a local development version thereof.[24] We employed DFT with the PBE0 exchange-correlation functional[25] using the multipole-accelerated resolution-of-the-identity (RI) approach.[26] A def2-TZVPP basis set[27] for the MCu_3O_6 core (M = Mn, Ni, Cu) and a def2-SVP basis set for the remaining atoms were used, together with appropriate fitting basis sets for the RI.[28] Grimme's D3 correction was employed to account for dispersion interactions.[29] At this level of theory, we performed unconstrained structure optimizations for the high-spin state of each of the three $M^{II}Cu^{II}_3$ star compounds **1**−**3** (only the isolated cations were considered). The def2-TZVPP basis set turned out to be important to reproducing Cu−O distances close to the experiment.

Magnetic couplings were extracted from broken-symmetry calculations for selected spin configurations.[30] We monitored the spin-expectation values, which do not deviate by more than 0.5% from the theoretical values for the corresponding true mixed-spin state.

UHF natural orbitals (NOs) were obtained from calculations with flipped spin on the central ion. These were turned into natural localized orbitals (NLOs) by applying a Pipek−Mezey-like localization procedure[31] to the predominantly singly occupied NOs. Orbitals were visualized using *MacMolPlt v7.4.3*.[32]

RESULTS AND DISCUSSION

Syntheses. The star compounds $[(Cu^{II}L)_3M^{II}](ClO_4)_2$ (**1**, M = Mn; **2**, M = Ni; **3**, M = Cu; **4**, M = Zn) were smoothly synthesized in reasonable yields upon reaction of the mononuclear copper(II) compound $[Cu^{II}L]$ with the appropriate metal perchlorate in a 3:1 stoichiometric ratio. It is interesting to mention that the same star compounds are produced if the stoichiometric ratio of the reactants is changed from 3:1 to 2:1, indicating that this ligand system has the potential to stabilize $M^{II}Cu^{II}_3$ star compounds rather than dinuclear $Cu^{II}M^{II}$ or trinuclear $Cu^{II}M^{II}Cu^{II}$ compounds when the second metal ion (M^{II}) is Mn^{II}, Ni^{II}, Cu^{II}, or Zn^{II}. We initiated the present work upon observing stabilization of a $[CdCu_3]^{2+}$ star compound[18a] derived from the same ligand system with the aim of exploring whether similar stars are isolated with bivalent 3d metal ions as the second metal ion. All in all, although it seems that H_2L is different from the closely similar ligands (where two imine nitrogen atoms are separated by two or three carbon atoms)[15] in terms of stabilization of the series of stars, it is not possible at this stage to explain the reason for such a difference or the peculiarity of H_2L.

Description of the Structures of 1−4. The structures of the four compounds $[(Cu^{II}L)_3M^{II}](ClO_4)_2$ (**1**, M = Mn; **2**, M = Ni; **3**, M = Cu; **4**, M = Zn) are shown in Figures 1−4, respectively. Each structure contains a $[(Cu^{II}L)_3M^{II}]^{2+}$ cation and two perchlorate anions, where the former is a metal-centered triangle or star in which the central metal ion is M^{II} and the three peripheral metal ions, i. e., the metal ions at the apexes of the triangle are three copper(II) ions. The central metal ion is linked with two μ_2-phenoxo bridges of each of the three $[Cu^{II}L]$ moieties and thus the central metal ion is hexacoordinated by six bridging phenoxo oxygen atoms and is encapsulated in between three $[Cu^{II}L]$ moieties. On the other

dx.doi.org/10.1021/ic501900d | Inorg. Chem. 2015, 54, 117−131

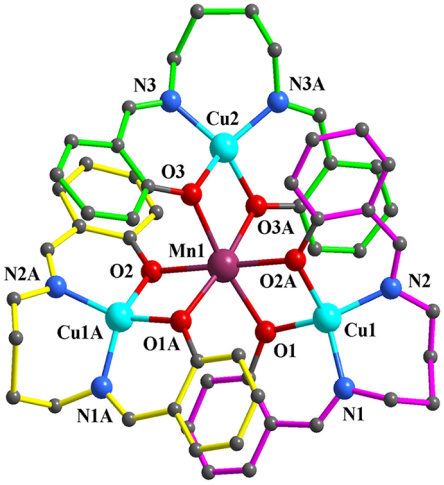

Figure 1. Crystal structure of $[Mn^{II}(Cu^{II}L)_3](ClO_4)_2$ (**1**). Hydrogen atoms and perchlorate anions are omitted for clarity. Symmetry code: A, 1.5 − *x*, *y*, 1 − *z*.

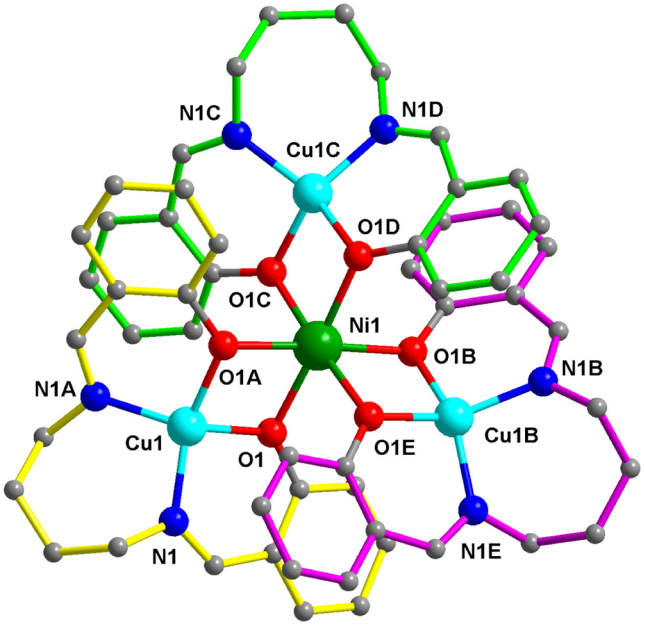

Figure 2. Crystal structure of $[Ni^{II}(Cu^{II}L)_3](ClO_4)_2$ (**2**). Hydrogen atoms and perchlorate anions are omitted for clarity. Symmetry codes: A, *y*, *x*, 0.5 − *z*; B, −*x* + *y*, −*x*, *z*; C, − *y*, *x* − *y*, *z*; D, −*x*, −*x* + *y*, 0.5 − *z*; E, *x* − *y*, −*y*, 0.5 − *z*.

hand, the peripheral copper(II) ion occupies $N(imine)_2O(phenoxo)_2$ compartment and is tetracoordinated by two imine nitrogen atoms and two bridging phenoxo oxygen atoms.

Half of the cluster in compounds **1**, **3**, and **4** is symmetry-related to the other half because of the presence of a crystallographic 2-fold axis passing through Mn1−Cu2, Cu3−Cu2, and Zn1−Cu2, respectively. On the other hand, compound **2** possesses trigonal symmetry. As a result, three M^{II}−phenoxo bonds in **1**, **3**, and **4** are symmetry-related to other three, while all six M^{II}−phenoxo bonds in **2** are equivalent. As expressed by the presence of a 2-fold axis in **1**, **3**, and **4** and trigonal symmetry in **2**, all four metal ions in the clusters lie in a plane. In the case of **1**, **3**, and **4**, the four metal ions form a centered isosceles triangle with the following parameter values: the apical angle (Cu1···Cu2···Cu1A) is 64.69° (**1**), 71.92° (**3**), and

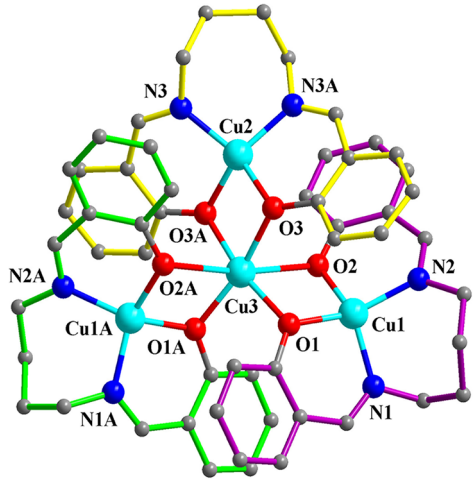

Figure 3. Crystal structure of $[Cu^{II}(Cu^{II}L)_3](ClO_4)_2$ (**3**). Hydrogen atoms and perchlorate anions are omitted for clarity. Symmetry code: A, 0.5 − *x*, *y*, 2 − *z*.

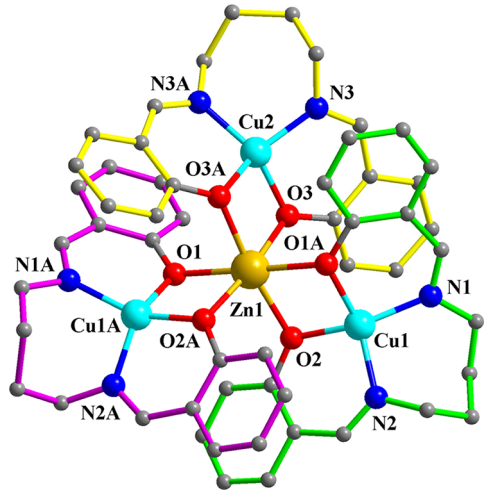

Figure 4. Crystal structure of $[Zn^{II}(Cu^{II}L)_3](ClO_4)_2$ (**4**). Hydrogen atoms and perchlorate anions are omitted for clarity. Symmetry code: A, 0.5 − *x*, *y*, 1 − *z*.

65.66° (**4**); the basal angle (Cu2···Cu1···Cu1A) is 57.66° (**1**), 54.04° (**3**), and 57.17° (**4**); the basal edge length (Cu1···Cu1A) is 5.705 Å (**1**), 5.935 Å (**3**), and 5.623 Å (**4**); the side edge length (Cu1···Cu2) is 5.331 Å (**1**), 5.053 Å (**3**), and 5.186 Å (**4**). On the other hand, the four metal ions in **2** form a centered equilateral triangle with edge length 5.274 Å.

Selected bond lengths and angles around the metal centers in **1**−**4** are listed in Table 2. The geometry of the central metal ion in each structure is distorted-octahedral. In comparison to the ideal values, the cis angles are more deviated than the trans angles: cis angle ranges are 73.15−106.58° (**1**), 76.63−100.92° (**2**), 71.97−114.58° (**3**), and 74.57−105.90° (**4**); trans angle ranges are 171.70−179.65° (**1**), 176.84° (**2**), 166.13−171.32° (**3**), and 172.09−179.39° (**4**). As usual, regarding the bond distances involving hexacoordinated Cu^{II}, the axial bond distances involving Cu3 in **3** are much longer (Cu3−O2/O2A = 2.431 Å) than the bond distances (1.972−2.022 Å) in the basal plane. The three types of central metal−phenoxo bond distances in **1** and **4** are 2.174/2.177/2.228 Å (Mn^{II}−O in **1**) and 2.095/2.103/2.172 Å (Zn^{II}−O in **4**), respectively, while the Ni^{II}−O bond distance in **2** is 2.086 Å.

dx.doi.org/10.1021/ic501900d | *Inorg. Chem.* 2015, 54, 117−131

Table 2. Selected Bond Lengths (Å) and Bond Angles (deg) for 1−4

1 ($Mn^{II}Cu^{II}_3$)		**2** ($Ni^{II}Cu^{II}_3$)		**3** ($Cu^{II}Cu^{II}_3$)		**4** ($Zn^{II}Cu^{II}_3$)	
Cu1−N1	1.919(4)	Cu1−N1	1.929(4)	Cu1−N1	1.930(3)	Cu1−N1	1.938(4)
Cu1−N2	1.913(5)	Cu1−O1	1.912(3)	Cu1−N2	1.943(3)	Cu1−N2	1.931(4)
Cu1−O1	1.919(3)	Ni1−O1	2.086(2)	Cu1−O1	1.944(2)	Cu1−O1A	1.909(2)
Cu1−O2A	1.925(3)	Ni1···Cu1	3.045	Cu1−O2	1.894(2)	Cu1−O2	1.915(3)
Cu2−O3	1.916(2)			Cu2−O3	1.914(2)	Cu2−O3	1.916(2)
Cu2−N3	1.923(3)			Cu2−N3	1.923(3)	Cu2−N3	1.925(3)
Mn1−O1	2.177(3)			Cu3−O1	1.972(2)	Zn1−O1	2.172(3)
Mn1−O2	2.228(3)			Cu3−O2	2.431(2)	Zn1−O2	2.095(2)
Mn1−O3	2.174(3)			Cu3−O3	2.022(2)	Zn1−O3	2.103(2)
Mn1···Cu1	3.168			Cu3···Cu1	3.169	Zn1···Cu1	3.099
Mn1···Cu2	3.126			Cu3···Cu2	2.978	Zn1···Cu2	3.054
N1−Cu1−O2A	143.45(16)	N1A−Cu1−O1	146.43(14)	N2−Cu1−O1	150.55(12)	N1−Cu1−O2	149.29(14)
N2−Cu1−O1	148.72(15)	N1−Cu1−O1	96.17(13)	N1−Cu1−O2	142.63(12)	N2−Cu1−O1A	142.37(14)
N3−Cu2−O3A	145.38(13)	N1−Cu1−N1A	100.6(2)	N3−Cu2−O3	145.80(12)	N3−Cu2−O3A	145.68(13)
N1−Cu1−N2	99.9(2)	O1−Cu1−O1A	85.13(14)	N1−Cu1−N2	100.70(14)	N1−Cu1−N2	100.52(18)
N2−Cu1−O2A	96.68(17)	O1−Ni1−O1D	176.84(13)	N2−Cu1−O2	96.87(12)	N2−Cu1−O2	95.98(15)
O1−Cu1−O2A	86.15(11)	O1−Ni1−O1E	81.59(14)	O2−Cu1−O1	85.80(10)	O2−Cu1−O1A	85.08(11)
O1−Cu1−N1	95.90(17)	O1−Ni1−O1A	76.63(13)	O1−Cu1−N1	94.37(12)	O1A−Cu1−N1	96.98(15)
N3−Cu2−O3	96.17(12)	O1−Ni1−O1C	100.92(9)	N3A−Cu2−O3	96.48(11)	N3−Cu2−O3	96.49(11)
O3−Cu2−O3A	86.58(15)			O3−Cu2−O3A	84.39(13)	O3−Cu2−O3A	85.73(13)
N3−Cu2−N3A	100.6(2)			N3−Cu2−N3A	101.26(17)	N3−Cu2−N3A	100.34(18)
O2−Mn1−O2A	179.65(15)			O2−Cu3−O2A	171.32(12)	O1−Zn1−O1A	179.39(13)
O1−Mn1−O3	171.70(10)			O1− Cu3−O3A	166.13(9)	O2−Zn1−O3A	172.09(9)
O2−Mn1−O1	106.58(11)			O1−Cu3−O2	71.97(9)	O1A−Zn1−O2	74.57(10)
O2−Mn1−O3A	99.07(10)			O1−Cu3−O2A	114.58(9)	O1A−Zn1−O3A	97.92(9)
O2−Mn1−O3	81.21(10)			O1−Cu3−O3	96.68(9)	O2−Zn1−O1	105.90(10)
O1−Mn1−O2A	73.15(10)			O1−Cu3−O1A	90.47(13)	O2A−Zn1−O1	74.57(10)
O1A−Mn1−O2A	106.57(11)			O2A−Cu3−O1A	71.97(8)	O3−Zn1−O1	97.91(9)
O3A−Mn1−O2	99.07(10)			O3A−Cu3−O1A	96.68(9)	O3A−Zn1−O1	81.60(9)
O1−Mn1−O1A	84.20(15)			O2−Cu3−O3	79.03(9)	O2−Zn1−O2A	85.17(14)
O3A−Mn1−O3	74.35(13)			O3−Cu3−O3A	78.95(12)	O3−Zn1−O3A	76.63(12)
O3A−Mn1−O1	101.12(10)			O3A−Cu3−O2	94.22(9)	O3−Zn1−O2	99.49(9)
Mn1−O1−Cu1	101.12(12)	Ni1−O1−Cu1	99.12(11)	Cu3−O1−Cu1	108.05(10)	Zn1−O1A−Cu1	98.60(11)
Mn1−O2A−Cu1	99.17(12)			Cu3−O2−Cu1	93.41(10)	Zn1−O2−Cu1	101.15(12)
Mn1−O3−Cu2	99.53(11)			Cu3−O3−Cu2	98.33(9)	Zn1−O3−Cu2	98.82(9)

The geometry of the peripheral copper(II) centers in the N_2O_2 compartment in **1**−**4** is highly distorted. If we consider the geometry as square planar, the range of cis angles in these environments is ca. 85−100° in all of **1**−**4** (Table 2), and the displacements (d_{Cu}) of the metal ion from the least-squares N_2O_2 basal plane lie in the range 0.000−0.055 Å, and so both of these parameters do not indicate much distortion. However, significant distortion is evidenced from the trans angles, which are smaller than the ideal value of 180° by ca. 29−38°, and also from the average deviation ($d_{N/O}$ ca. 0.55 Å) of the constituent nitrogen and oxygen atoms from the least-squares N_2O_2 plane. To quantify and evaluate the distortion from the ideal square-planar or ideal tetrahedral coordination, shape analysis has been done with the routine *SHAPE*.[33] The geometry of the copper(II) ions in **1** corresponds to 52.3%/51.3% to a square-planar coordination and to 47.7%/48.7% to a tetrahedral coordination, respectively, lying closely in the middle of both coordination modes following the ideal path between a square-planar and tetrahedral coordination. From this, it is evident that the copper(II) ions have an intermediate coordination environment between an ideal square-planar and ideal tetrahedral coordination. The geometry of the peripheral copper(II) centers in other complexes is also similarly distorted, with values corresponding to 52.8% (47.2%) for **2**, 52.9%/52.0% (47.1%/48.0%) for **3**, 51.8%/51.7% (48.2%/48.3%) for **4** to an ideal square-planar (tetrahedral) coordination.

Three types of Cu−O(phenoxo)−Mn bridge angles in **1** are not very different (Cu1−O1−Mn1 = 101.12°, Cu1−O2A−Mn1 = 99.17°, and Cu2−O3−Mn1 = 99.53°), as are the three types of Cu−O−Zn angles in **4** (Cu1−O1A−Zn1 = 98.60°, Cu1−O2−Zn1 = 101.15°, and Cu2−O3−Zn1 = 98.82°). One type of Cu−O−Ni phenoxo bridge angle in **2** is 99.12°. On the other hand, three types of Cu−O−Cu phenoxo bridge angles in **3** are significantly different (Cu1−O1−Cu3 = 108.05°, Cu1−O2−Cu3 = 93.41°, and Cu2−O3−Cu3 = 98.33°). The distance between the central and peripheral metal ions in **1**−**4** lies in the range 2.978−3.169 Å (Table 2).

It is relevant to mention the structural importance of compounds **1**−**4**. Previously, several star-shaped molecules have been reported where the three central···peripheral metal ion pairs are bridged by two monatomic alkoxo/hydroxo/phenoxo/oxo/carboxylate/methoxide bridges.[15,18a,19b−d,22,34] Most of those are homometallic tetranuclear systems such as Fe^{III}_4, Mn^{II}_4, Cr^{III}_4, Co^{III}_4, Co^{II}_4, $Co^{II}Co^{III}_3$, etc.[15,34] On the other hand, star-shaped heterometallic complexes are just a few and include the following metal-ion combinations: $Mn^{III}Co^{III}_3$,

dx.doi.org/10.1021/ic501900d | *Inorg. Chem.* 2015, 54, 117−131

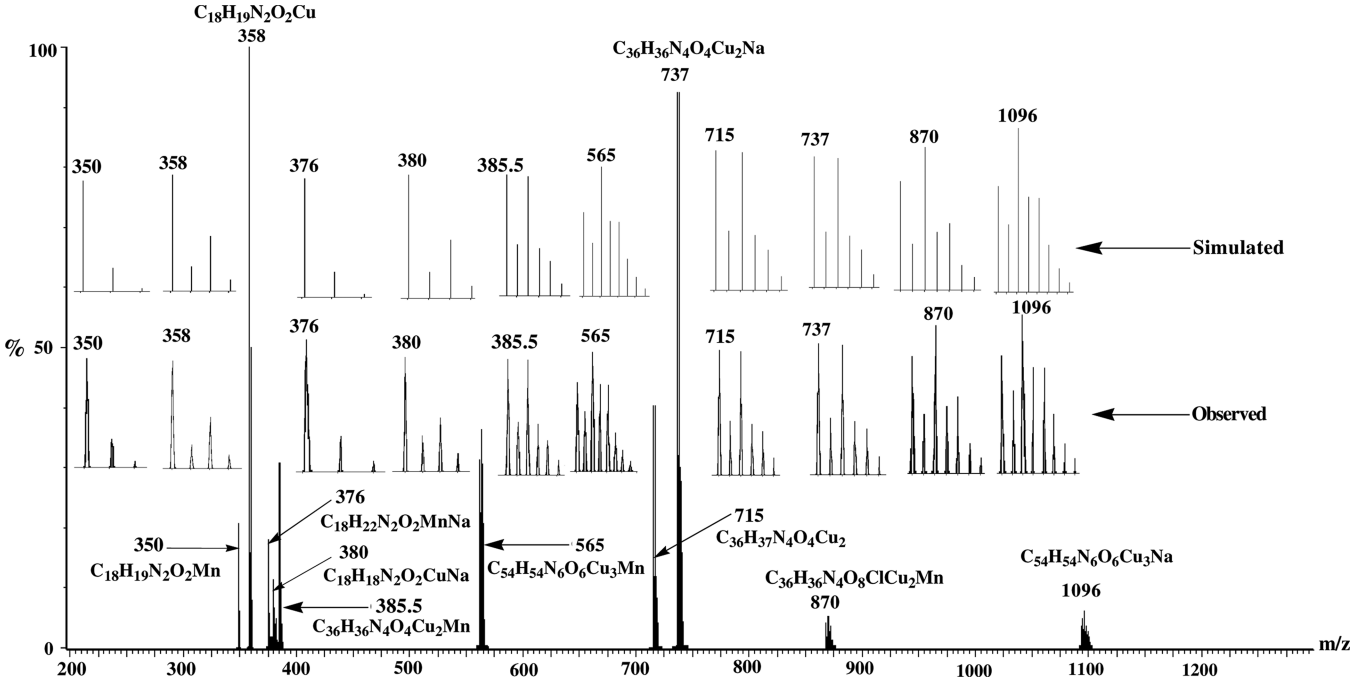

Figure 5. Positive-mode ESI-MS spectrum of **1** in acetonitrile showing the observed and simulated isotopic distribution patterns.

Table 3. Composition, Formula, Formula Weight, *m/z* Values, and Intensity of the Positive Ions Identified in Positive-Mode ESI-MS Spectra of 1–4[a]

composition, formula of ions	*m/z*, intensity (*I*, %), and line-to-line separation (Δ_1)			
	1	**2**	**3**	**4**
$[Cu^{II}L{\cdot}H^+]^+$ (**I**), $C_{18}H_{19}N_2O_2Cu$	358, 100, 1.0	358, 30, 1.0	358, 100, 1.0	358, 100, 1.0
$[M^{II}L{\cdot}H^+]^+$ (**II**), $C_{18}H_{19}N_2O_2M$	350, 20, 1.0	353, 100, 1.0		
$[Na^{I}L{\cdot}2H^+]^+$ (**III**), $C_{18}H_{20}N_2O_2Na$			319, 25, 1.0	
$[Cu^{II}LNa^{I}]^+$ (**IV**), $C_{18}H_{18}N_2O_2CuNa$	380, 12, 1.0		380, 20, 1.0	380, 62, 1.0
$[Mn^{II}L^{s}Na^{I}]^+$ (**V**),[b] $C_{18}H_{22}N_2O_2MnNa$	376, 18, 1.0			
$[(Cu^{II}L)_2{\cdot}H^+]^+$ (**VI**), $C_{36}H_{37}N_4O_4Cu_2$	715, 40, 1.0	715, 10, 1.0	715, 15, 1.0	715, 25, 1.0
$[(Cu^{II}L)_2Na^{I}]^+$ (**VII**), $C_{36}H_{36}N_4O_4Cu_2Na$	737, 90, 1.0	737, 25, 1.0	737, 60, 1.0	737, 55, 1.0
$[(Cu^{II}L)_2M^{II}]^{2+}$ (**VIII**), $C_{36}H_{36}N_4O_4Cu_2M$	385.5, 30, 0.5	388, 92, 0.5		
$[(Cu^{II}L)_2M^{II}(ClO_4)]^+$ (**IX**), $C_{36}H_{36}N_4O_8ClCu_2M$	870, 6, 1.0	873, 6, 1.0		
$[M^{II}(Cu^{II}L)_3]^{2+}$ (**X**), $C_{54}H_{54}N_6O_6Cu_3M$	565, 35, 0.5	566.5, 6, 0.5		
$[Na^{I}(Cu^{II}L)_3]^+$ (**XI**), $C_{54}H_{54}N_6O_6Cu_3Na$	1096, 6, 1.0		1096, 5, 1.0	1096, 6, 1.0

[a] *m/z* values quoted in this table are for the major peak in the isotope pattern. [b] $[L^s]^{2-}$ is the saturated diamine analogue of [L].

$Zn^{II}Co^{III}_3$, $Ni^{II}Co^{III}_3$, $Co^{II}Cr^{III}_3$, $Cr^{III}Fe^{III}_3$, $Cd^{II}Cu^{II}_3$, $Na^{I}Cu^{II}_3$, and $Mn^{II}Cu^{II}_3$.[15,18a,19b–d,22] The $Mn^{II}Cu^{II}_3$ compound **1** is the second such star,[19b] while the $Ni^{II}Cu^{II}_3$ (**2**), $Cu^{II}Cu^{II}_3$ (**3**), and $Zn^{II}Cu^{II}_3$ (**4**) are the sole examples of such star-shaped molecules. Again, compounds **1**–**4** are among only a few examples of star-shaped systems derived from Schiff base ligands.[18a,19b,c]

In most of the heterometallic star-shaped systems except one $Cd^{II}Cu^{II}_3$ complex,[18a] the difference in the central metal–O bond distances is rather high. It is relevant to mention at this point the central metal–phenoxo bond distances in the previously reported few examples of star-shaped complexes derived from Schiff base ligands. The metal–O distances in those complexes vary widely between 2.116 and 2.324 Å in the only $Mn^{II}Cu^{II}_3$ complex, between 2.242 and 2.819 Å in the only $Na^{I}Cu^{II}_3$ complex, and between 2.212 and 2.410 Å in one of the two $Cd^{II}Cu^{II}_3$ complexes.[19b–d] Because the crystal system/space group of **2** is trigonal/$P\bar{3}c1$, it is a highly symmetric molecule, and therefore all six Ni^{II}–O(phenoxo) bond distances are equal at 2.086 Å. In heterometallic stars, such equality of all six bond distances takes place only in the $Cd^{II}Cu^{II}_3$ compound derived from the same ligand, H_2L.[18a] Compound **2** is therefore only the second example of the two best star systems. The $Mn^{II}Cu^{II}_3$ compound **1** is also a better star than its only analogue;[19b] the ranges of Mn^{II}–O bond distances in two are 2.177–2.228 and 2.116–2.324 Å, respectively. The Zn^{II}–O bond distances also lie in a narrower range, 2.095–2.172 Å. On the other hand, because of the usual Jahn–Teller distortion, the range of Cu^{II}–O bond distances in the $Cu^{II}Cu^{II}_3$ star is rather wide, 1.972–2.431 Å.

ESI-MS and UV–Vis Studies. The positive-mode ESI-MS spectra of acetonitrile solutions of compounds **1**–**4** were recorded. The observed and simulated spectra of **1**–**4** are shown in Figures 5 and S1–S3 in the Supporting Information (SI), respectively, while the formula/formula weight, *m/z*, intensity, and line-to-line separation of the species that correspond to all of the observed peaks of all four compounds are listed in Tables 3 (without drawing) and S1 in the SI (with drawing).

dx.doi.org/10.1021/ic501900d | Inorg. Chem. 2015, 54, 117–131

The isotropic distributions of the observed and simulated peaks are matched well. A total of 11 types of species (**I**–**XI**) are observed in the spectra of **1**–**4**. Three among the 11 species are mononuclear: (i) $[Cu^{II}L{\cdot}H^{+}]^{+}$ (**I**; for all four complexes); (ii) $[M^{II}L.H^{+}]^{+}$ [**II**; for **1** (M = Mn) and **2** (M = Ni) only]; (iii) $[Na^{I}L{\cdot}2H^{+}]^{+}$ (**III**; only for **3**). Three among the 11 species are possibly dinuclear: (i) $[Cu^{II}LNa^{I}]^{+}$ (**IV**; for **1**, **3**, and **4**); (ii) $[Mn^{II}L^{s}Na^{I}]^{+}$ (**V**; for **1** only; $[L^{s}]^{2-}$ is the saturated diamine analogue of $[L]^{2-}$); (iii) $[(Cu^{II}L)_2{\cdot}H^{+}]^{+}$ (**VI**; for all four complexes). Three among the 11 species are possibly trinuclear: (i) $[(Cu^{II}L)_2Na^{I}]^{+}$ (**VII**; for all four complexes); (ii) $[(Cu^{II}L)_2M^{II}]^{2+}$ [**VIII**; for **1** (M = Mn) and **2** (M = Ni)]; (iii) $[(Cu^{II}L)_2M^{II}(ClO_4)]^{+}$ [**IX**; for **1** (M = Mn) and **2** (M = Ni)]. Two among the 11 species are possibly tetranuclear star systems: (i) $[M^{II}(Cu^{II}L)_3]^{2+}$ [**X**; for **1** (M = Mn) and **2** (M = Ni)]; (ii) $[Na^{I}(Cu^{II}L)_3]^{+}$ (**XI**; for **1**, **3**, and **4**). The salient features are as follows: (i) the mononuclear Cu^{II} species $[Cu^{II}L{\cdot}H^{+}]^{+}$ (**I**), dinuclear Cu^{II}_2 species $[(Cu^{II}L)_2{\cdot}H^{+}]^{+}$ (**VI**), and trinuclear $Cu^{II}Na^{I}Cu^{II}$ species $[(Cu^{II}L)_2Na^{I}]^{+}$ (**VII**) appear in the spectra of all four compounds; (ii) the spectra of the $Mn^{II}Cu^{II}_3$ compound **1** and $Ni^{II}Cu^{II}_3$ compound **2** are similar to each other, and both are different from those of the $Cu^{II}Cu^{II}_3$ compound **3** and $Zn^{II}Cu^{II}_3$ compound **4** in terms of the appearance of the following species in the case of the former but not in the case of the latter—the mononuclear $[M^{II}L{\cdot}H^{+}]^{+}$ (**II**; M = Mn, Ni), trinuclear $Cu^{II}M^{II}Cu^{II}$ species $[(Cu^{II}L)_2M^{II}]^{2+}$ (**VIII**) and $[(Cu^{II}L)_2M^{II}(ClO_4)]^{+}$ (**IX**), and the tetranuclear star species $[M^{II}(Cu^{II}L)_3]^{2+}$ (**X**); (iii) a tetranuclear star species $[Na^{I}(Cu^{II}L)_3]^{+}$ (**XI**) and a dinuclear $Cu^{II}Na^{I}$ species $[Cu^{II}LNa^{I}]^{+}$ (**IV**) appear in the spectra of the $Mn^{II}Cu^{II}_3$ compound **1**, $Cu^{II}Cu^{II}_3$ compound **3**, and $Zn^{II}Cu^{II}_3$ compound **4** but not in the $Ni^{II}Cu^{II}_3$ compound **2**; (iv) a mononuclear Na^{I} species $[Na^{I}L{\cdot}2H^{+}]^{+}$ (**III**) appears in the spectrum of only the $Cu^{II}Cu^{II}_3$ compound **3**; (v) a saturated diamine analogue is observed only in the spectrum of the $Mn^{II}Cu^{II}_3$ compound **1**, and the corresponding species is $[Mn^{II}L^{s}Na^{I}]^{+}$ (**V**). Clearly, the original star dication of composition $[M^{II}(Cu^{II}L)_3]^{2+}$ is observed in two cases (M = Mn, Ni) but not in two other cases (M = Cu, Zn); i.e., $[Mn^{II}(Cu^{II}L)_3]^{2+}/[Ni^{II}(Cu^{II}L)_3]^{2+}$ is stable but $[Cu^{II}(Cu^{II}L)_3]^{2+}/[Zn^{II}(Cu^{II}L)_3]^{2+}$ is not stable in the time scale of positive-mode ESI-MS spectra. It is worth mentioning in this context that the appearance of the ions, original or others, and hence the fragmentation pattern in ESI-MS are a property of an individual compound.

UV–vis spectra of the acetonitrile solutions of the mononuclear compound $[Cu^{II}L]$ and compounds **1**–**4** were recorded. The spectra are shown in Figures S4 and S5 in the SI, while the absorption positions and extinction coefficients are listed in Table S2 in the SI. A band for each of the $[Cu^{II}L]$ (647 nm, 234 M^{-1} cm^{-1}), $Mn^{II}Cu^{II}_3$ compound **1** (611 nm, 302 M^{-1} cm^{-1}), $Ni^{II}Cu^{II}_3$ compound **2** (628 nm, 337 M^{-1} cm^{-1}), and $Zn^{II}Cu^{II}_3$ compound **4** (609 nm, 313 M^{-1} cm^{-1}), as well as a shoulder for the $Cu^{II}Cu^{II}_3$ compound **3** (630 nm, 478 M^{-1} cm^{-1}), can be assigned to the d–d transition of the copper(II) centers. All five compounds exhibit a strongly intense band, with the band maximum and extinction coefficient lying in the ranges 352–374 nm and 10066–28748 M^{-1} cm^{-1}, respectively, which probably correspond to the superposition of the internal ligand transition and phenoxo → metal ion charge-transfer transition. A shoulder around 300 nm with an extinction coefficient in the range 7685–23012 M^{-1} cm^{-1} is observed in the spectra of $[Cu^{II}L]$, **2**, and **3** but not in those of **1** and **4**. This last absorption arises because of the internal ligand transition. The characteristic transitions for six-coordinated nickel(II) in **2** are not observed/identified. The higher-energy transitions are probably merged with the d–d absorption of copper(II) and internal ligand transitions, while the possible near-IR transition of low intensity could not be observed because of low solubility.

Magnetic Properties of 1–4. Variable-temperature (2–300 K) magnetic properties of complexes **1**–**4** are shown in Figures 6–8 and S6 in the SI, respectively. For the

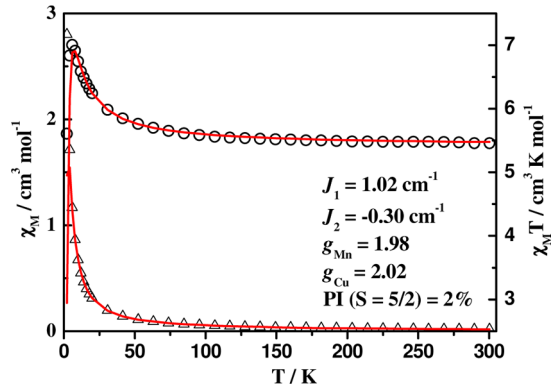

Figure 6. Fittings of $\chi_M T/\chi_M$ versus T of **1** between 2 and 300 K. The experimental data are shown as black symbols, and the red lines correspond to the theoretical values, listed in the inset, where J_1 and J_2 are respectively central···peripheral (Mn^{II}···Cu^{II}) and peripheral···peripheral (Cu^{II}···Cu^{II}) exchange integrals.

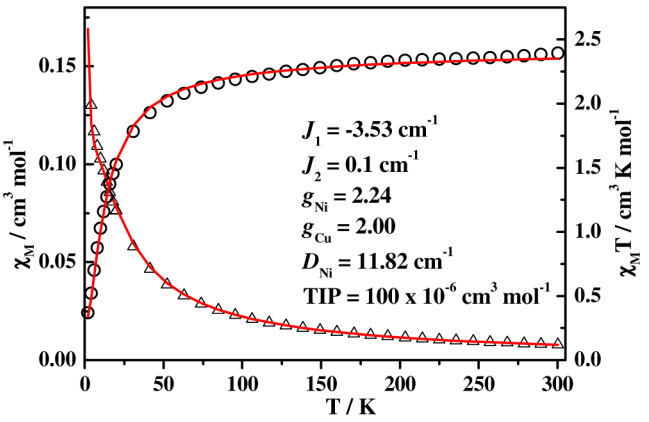

Figure 7. Fittings of $\chi_M T/\chi_M$ versus T of **2** between 2 and 300 K. The experimental data are shown as black symbols, and the red lines correspond to the theoretical values, listed in the inset, where J_1 and J_2 are respectively central···peripheral (Ni^{II}···Cu^{II}) and peripheral···peripheral (Cu^{II}···Cu^{II}) exchange integrals.

$Mn^{II}Cu^{II}_3$ compound **1**, the $\chi_M T$ value at room temperature is 5.46 cm^3 K mol^{-1}, which is very close to the expected value of 5.50 cm^3 K mol^{-1} for four uncoupled spins with $S_1 = {}^5/_2$ and $S_2 = S_3 = S_4 = {}^1/_2$. Upon lowering of the temperature to 6 K, a smooth increase of the $\chi_M T$ value to 7.00 cm^3 K mol^{-1} is observed. Further cooling leads to a decrease of the $\chi_M T$ product, reaching a value of 5.60 cm^3 K mol^{-1} at 2 K. The profile indicates ferromagnetic interaction. The $\chi_M T$ value of the $Ni^{II}Cu^{II}_3$ compound **2** at room temperature is 2.39 cm^3 K mol^{-1}, which is slightly higher than the expected value of 2.12 cm^3 K mol^{-1} for four uncoupled spins with $S_1 = 1$ and $S_2 = S_3 = S_4 = {}^1/_2$. Upon lowering of the temperature to 2 K, a smooth decrease of the $\chi_M T$ value to 0.37 cm^3 K mol^{-1} is observed, indicating antiferromagnetic interaction between the nickel(II) and copper(II) ions. For the $Cu^{II}Cu^{II}_3$ compound **3** at room temperature, a $\chi_M T$ value of

dx.doi.org/10.1021/ic501900d | Inorg. Chem. 2015, 54, 117–131

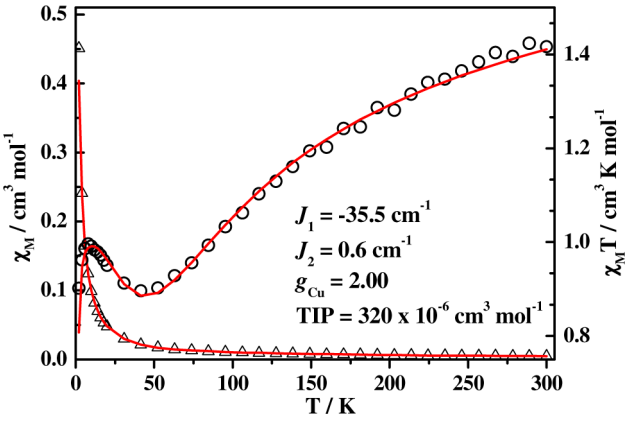

Figure 8. Fittings of $\chi_M T/\chi_M$ versus T of **3** between 2 and 300 K. The experimental data are shown as black symbols, and the red lines correspond to the theoretical values, listed in the inset, where J_1 and J_2 are respectively central···peripheral (Cu^{II}···Cu^{II}) and peripheral···peripheral (Cu^{II}···Cu^{II}) exchange integrals.

1.42 cm^3 K mol^{-1} is observed, which is slightly lower than the expected value of 1.50 cm^3 K mol^{-1} for four uncoupled spins with $S_1 = S_2 = S_3 = S_4 = {}^1/_2$. Upon lowering of the temperature to 40 K, the $\chi_M T$ value decreases to 0.88 cm^3 K mol^{-1}. Further cooling leads first to an increase to 0.99 cm^3 K mol^{-1} at 10 K and then to a rapid decrease, reaching a value of 0.81 cm^3 K mol^{-1} at 2 K. The steady decrease of $\chi_M T$ upon lowering of the temperature from 300 to 40 K is indicative of antiferromagnetic interaction. The variable-temperature susceptibility data of the $Zn^{II}Cu^{II}_3$ compound **4** (Figure S6 in the SI) shows the $\chi_M T$ values remaining practically unchanged at ca. 1.28 cm^3 K mol^{-1} in the temperature range 300–40 K. Below 40 K, a decrease of $\chi_M T$ is observed to 0.025 cm^3 K mol^{-1} at 2 K. The profile indicates very weak antiferromagnetic interaction between the copper(II) centers, of intra- or intermolecular nature.

In compounds **1**–**3**, dominant magnetic exchange take place between the central metal ion with each of the three peripheral copper(II) ions through bis(μ_2-phenoxo) bridges, while the interaction between the peripheral copper(II) ions should be small. According to established magnetostructural correlations in different types of diphenoxo/alkoxo/dihydroxo bridged systems, the metal–O–metal bridge angle (α) is the most crucial parameter to govern the nature and magnitude of magnetic exchange interactions.[8,9a,10a,11,12,13a] The metal–O–metal–O torsion angles (τ) and out-of-plane shift (φ) of the phenyl groups should also have some definite roles in the magnetic properties of diphenoxo-bridged systems.[13a] In the $Mn^{II}Cu^{II}_3$ compound **1**, averages of these parameters for Cu1/Cu1A···Mn1 and Cu2···Mn1 pairs are respectively 100.15 and 99.53° (α), 4.62 and 0.00° (τ), and 21.67 and 20.13° (φ). Because these three parameters are not very different for the two types of routes, it is logical to consider the same magnetic exchange integral for all three spin pairs. On the other hand, the situation is different for the $Cu^{II}Cu^{II}_3$ compound **3**. Average values of α, τ and φ are not much different for the Cu1/Cu1A···Cu3 (α = 100.73°, τ = 6.41°, and φ = 19.98°) and Cu2···Cu3 (α = 98.33°, τ = 0.00°, and φ = 18.66°) pairs. However, one phenoxo bridge (O2) is axial–equatorial and the second (O1) is equatorial–equatorial for the Cu1/Cu1A···Cu3 pair, while both the phenoxo bridges (O3 and O3A) are equatorial–equatorial for the Cu2···Cu3 pair. Thus, while the axial–equatorial route (O2) with phenoxo bridge angle 93.41° should mediate ferromagnetic exchange, the equatorial–equatorial route (O1) with phenoxo bridge angle 108.05° should mediate strong antiferromagnetic exchange. On the other hand, for the second pair (Cu2···Cu3), both equatorial routes (O3 and O3A) with phenoxo bridge angle 98.33° should mediate moderate antiferromagnetic exchange.

For **1** and **3**, an exchange interaction model with two different central---peripheral coupling constants was taken into account. However, no significant differences can be observed. Consequently, to minimize the number of parameters avoiding overparametrization, only one coupling constant between the central metal and the peripheral copper(II) ions was taken into account. This is in accordance with the very similar bridging mode in **1**, while in **3**, the different routes over O2 mediating ferromagnetic exchange, O1 mediating strong antiferromagnetic exchange, and O3 mediating moderate antiferromagnetic exchange are balancing each other, resulting in comparable strength of the coupling constants. Because of trigonal symmetry in the $Ni^{II}Cu^{II}_3$ compound **2**, the three central···peripheral exchange integrals in this compound are clearly the same. Thus, for all three complexes, a similar model Hamiltonian (eq 1 according to Chart 2) was used, where three central···peripheral

Chart 2. Model of Magnetic Exchange in 1–3

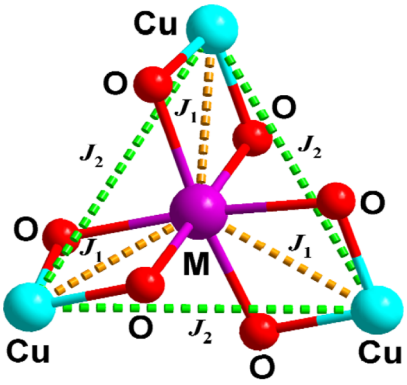

[M^{II}···Cu^{II}; M = Mn (**1**), Ni (**2**), and Cu (**3**)] interactions are the same (J_1) and also the three peripheral···peripheral (Cu^{II}···Cu^{II}) interactions are the same (J_2). Additionally, the single-ion zero-field effect (D_{Ni}) of the Ni^{II} ion for **2**, temperature-independent paramagnetism (TIP) for compounds **2** and **3**, and a paramagnetic impurity (PI) for compound **1** were taken into account in the simulation of magnetic susceptibility data.

$$H = -2J_1(S_1\cdot S_2 + S_1\cdot S_3 + S_1\cdot S_4) - 2J_2(S_2\cdot S_3 + S_2\cdot S_4 + S_3\cdot S_4) + g_1\beta S_1\cdot B + g_2\beta(S_2\cdot B + S_3\cdot B + S_4\cdot B) \quad (1)$$

Simulations of magnetic data were carried out with the *PHI* program, which allows for a simultaneous susceptibility/magnetization fit.[35] As shown in Figures 6–8 and S6 in the SI for the susceptibility data and in Figures 9 and S7 and S8 in the SI for the magnetization data (2–10 K), contemporaneously good-quality fittings are obtained with the following converging parameters: J_1 = 1.02(1) cm^{-1}, J_2 = −0.30(3) cm^{-1}, g_{Cu} = 2.02, g_{Mn} = 1.98, and PI ($S = {}^5/_2$) = 2% for **1** ($Mn^{II}Cu^{II}_3$); J_1 = −3.53(9) cm^{-1}, J_2 = +0.1(2) cm^{-1}, g_{Cu} = 2.00, g_{Ni} = 2.24(4), D_{Ni} = 11.82 cm^{-1}, and TIP = 100 × 10^{-6} cm^3 mol^{-1} for **2** ($Ni^{II}Cu^{II}_3$); J_1 = −35.5(10) cm^{-1}, J_2 = +0.6(3) cm^{-1},

dx.doi.org/10.1021/ic501900d | *Inorg. Chem.* 2015, 54, 117–131

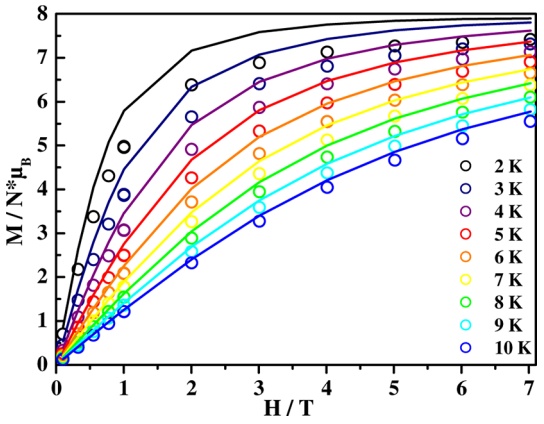

Figure 9. Low-temperature magnetization of **1** obtained at the indicated applied direct-current fields. The symbols are the experimental data, while the solid lines represent the calculated curves, with the parameters listed in the inset of Figure 6.

g_{Cu} = 2.00, and TIP = 320 × 10^{-6} cm^3 mol^{-1} for **3** ($Cu^{II}Cu^{II}_3$); J_2 = −1.4(3) cm^{-1} and g_{Cu} = 2.16(1) for **4** ($Zn^{II}Cu^{II}_3$). From the simulations, information regarding the lowest-lying spin states is as follows: for the $Mn^{II}Cu^{II}_3$ compound **1**, the ground state is S = 4 from which the first excited state (S = 3, 2-fold degenerate) is separated only by 4.2 cm^{-1}; for the $Ni^{II}Cu^{II}_3$ compound **2**, the ground state is S = 0.5 from which the first excited state (S = 1.5) is separated only by 7.3 cm^{-1}; for the $Cu^{II}Cu^{II}_3$ compound **3**, the ground state is S = 1 from which the first excited state (S = 0, 2-fold degenerate) is separated by 37.5 cm^{-1}.

Including compound **1**, there are 19 compounds where copper(II) and manganese(II) centers are bridged by solely the bis(μ_2-phenoxo) moiety.[18c−f,19b,36,37] These compounds (**I**−**XVIII** and **1**) along with the values of magnetic and possible governing parameters are listed in Table 4. Those types of compounds are dinuclear; dimer-of-dinuclear; tetranuclear; cocrystal of one dinuclear $Cu^{II}Mn^{II}$ and two mononuclear Cu^{II}; and polymeric where dinuclear $Cu^{II}Mn^{II}$ units are bridged by inorganic or organic bridging ligands such as tetracyanometalate(II), pyrazoledicarboxylate, oxalate, and benzene-1,3,5-tricarboxylate. However, it has been possible to determine the exchange integral in the Cu^{II}bis(μ_2-phenoxo)-Mn^{II} moiety in all of those compounds. It is quite impossible to find any correlation of the J values with the Cu^{II}−phenoxo, Mn^{II}−phenoxo, and $Cu^{II}\cdots Mn^{II}$ distances. For these compounds, in general, the interaction is more antiferromagnetic, with J values ranging between −24.45 and −36.8 cm^{-1} for larger phenoxo bridge angles (105.25−107.11°; compounds **I**−**V**), while the interaction is less antiferromagnetic, with J values ranging between −6.35 and −20.25 cm^{-1} for smaller phenoxo bridge angles (95.7−103.75°; compounds **VI**−**XII** and **XIV**−**XVII**). However, the J versus α relationship is not linear; i.e., the correlation is not straightforward (Figure S9 in the SI). Both τ and φ values in **I**−**IX** are smaller, while either or both of these values are greater for other compounds. However, their effects are also not straightforward (Figures S10 and S11 in the SI).

Interestingly, compound **1** in the present investigation is the sole example of a diphenoxo-bridged $Cu^{II}Mn^{II}$ system exhibiting ferromagnetic interaction (J = 1.02 cm^{-1}). Moreover, to the best of our knowledge, this is the sole example of showing ferromagnetic interaction between copper(II) and manganese(II) where metal ions are bridged by only one or more oxo bridge (phenoxo/hydroxo/alkoxo) or by a heterobridging moiety having oxo bridge(s) and some other bridges. As already mentioned, there is only one more $Mn^{II}Cu^{II}_3$ star (compound **XVIII**[18b] in Table 4), and therefore it is more relevant to compare **1** with **XVIII**. Two of the three J values in **XVIII** are the same, −20.25 cm^{-1}, for α = 99.50/99.93°, φ = 29.88/35.65°, and τ = 20.54/15.69°. In comparison, the α values (99.53/100.15°) in **1** are very close to those in **XVIII** and both the φ (20.13/21.67°) and τ (0.00/4.62°) values in **1** are smaller or significantly smaller than those in **XVIII**. Clearly, in comparison to two J values of −20.25 cm^{-1} in **XVIII**, the J values in **1** should be more antiferromagnetic. Not only that, in comparison to the third J = −6.35 cm^{-1} in **XVIII** for α = 96.85°, φ = 26.48°, and τ = 18.09°, the ferromagnetic interaction in **1** is more unusual.

It is therefore relevant to rationalize the origin of such unusual interaction in **1**. It is also clear that the parameter values around the manganese(II) environment cannot shed light on such unusual behavior. Therefore, we have looked into the coordination environment of three peripheral copper(II) ions. It has already been discussed that the environment of the peripheral copper(II) center in **1**−**3** is highly distorted and intermediate between square-planar and tetrahedral geometry, where the ranges of weight of the square-planar and tetrahedral geometry are 51.3−52.9% and 47.1−48.7%, respectively. On the other hand, the environment of copper(II) in the previously published compounds **I**−**XVIII** (Table 4) is either distorted square planar, distorted square pyramidal, or distorted octahedral, but the extent of distortion is small. For the tetracoordinated copper(II) in some of the systems among **I**−**XVIII**, a direct comparison in terms of the weight of the square-planar and tetrahedral geometry is possible from shape analysis with the routine *SHAPE*.[33] In those cases, the weight of the square-planar geometry lies in the range 81.6−92.1%, clearly indicating that environments are slightly distorted square planar. In the case of the pentacoordinated copper(II) ions, the values of the τ parameter were estimated to quantify distortion from the ideal polyhedral; a value of 0 is tantamount to the ideal square-pyramidal coordination and a value of 1 the trigonal-bipyramidal geometry, respectively.[38] The values of the τ parameter of pentacoordinated copper(II) in the systems among **I**−**XVIII** range from 0 to 0.18, which are very close to the ideal values for the square-pyramidal coordination geometry. Again, an idea about the extent of distortion can be obtained from a comparison of some structural parameters in the basal plane. A comparison of some structural parameters of the peripheral copper(II) environment (Table 4) reveals that compound **1** is an odd member in terms of significantly smaller transoid angles (143.45−148.72° in **1**; 158.78−178.67° in all others) and $d_{N/O}$ values (0.544 and 0.554 Å in **1**; 0.000−0.186 Å in all others), reflecting unusually significant distortion of the coordination environment of the peripheral copper(II) ion in **1**. Hence, it seems that unusually large distortion of the coordination environment of copper(II) is the reason for the unusual ferromagnetic behavior between copper(II) and manganese(II) in **1**.

Magnetic and some relevant structural parameters of all of the structurally characterized compounds in which the copper(II) and nickel(II) centers are bridged by solely the bis(μ_2-phenoxo) moiety are listed in Tables 5 and S4 in the SI.[39,40] In spite of having different types of nuclearity or in spite of the presence of other metal ions in some cases, the magnetic exchange integral between copper(II) and nickel(II) through the

dx.doi.org/10.1021/ic501900d | *Inorg. Chem.* 2015, 54, 117−131

Table 4. Magnetic Exchange Integral and Some Relevant Structural Parameters of All Systems Where Copper(II) and Manganese(II) Are Bridged Solely by the Bis(μ_2-phenoxo) Moiety

							peripheral copper(II)			
compd no.	CSD code	compd type	J (cm^{-1})	Cu−O−Mn (α, deg)[e]	φ (deg)[e,f]	Cu−O−Mn−O (τ, deg)[e]	cis angle range (deg)	trans angle range (deg)	d_{Cu}(Å)	d_{NO}(Å)[e]	ref
I[a]	GAJYOH	$Cu^{II}Mn^{II}$-based polymer	−36.8	107.11	10.75	3.36	77.48−98.36	164.01−167.86	0.145	0.078	36a
II[a]	VOBLAA	$Cu^{II}Mn^{II}$-based polymer	−32.35	106.77, 105.98, 105.25	7.32, 4.86, 3.1	3.00, 3.19, 8.93	78.18−98.73, 79.16−97.74, 78.44−99.32	168.23−169.59, 168.76−170.87, 158.78−169.59	0.068, 0.063, 0.182	0.022, 0.036, 0.127	36b
III[a]	VOBLII	$Cu^{II}Mn^{II}$-based polymer	−30.2	106.51	8.51	8.21	77.97−98.77	167.79−168.86	0.082	0.039	36b
IV[b]		$Cu^{II}Mn^{II}$	−29.1	106.90	2.54	5.82	77.36−97.60	169.69−169.94	0.019	0.007	18c
V[c]	VOBKUT	$Cu^{II}Mn^{II}$-based polymer	−24.45	106.34	5.96	2.07	78.47−98.15	166.29−170.05	0.059	0.099	36b
VI[c]	DEXQUT	$Cu^{II}Mn^{II}\cdots 2Cu^{II}$	−14	103.75	5.69	0.00	82.95−95.11	177.69	0.000	0.021	18d
VII[c]	YUVRAJ	$Cu^{II}Mn^{II}\cdots 2Cu^{II}$	−15.1	103.75	5.62	2.41	82.82−95.23	177.88−178.01	0.000	0.007	18e
VIII[c]	MIXLEL	$Cu^{II}Mn^{II}\cdots 2Cu^{II}$	−15.9	103.42	6.47	3.43	83.56−95.35	178.53−178.67	0.005	0.007	18f
IX[c]		$Cu^{II}Mn^{II}\cdots 2Cu^{II}$	−15.9	102.66	6.80	8.27	82.85−96.18	178.05−178.19	0.008	0.017	18c
X[c]	ILAKOV	$(Cu^{II}Mn^{II})_2$	−11.0	101.61	7.55	11.72	83.71−96.71	173.53−176.11	0.034	0.073	36c
XI[a]	QEKFIW	$Cu^{II}Mn^{II}$	−18.4	100.9	14.23	9.79	83.44−95.67	164.38−174.16	0.083	0.176	36d
XII[c]	LEGJAI	$Cu^{II}Mn^{II}$	−11.0	100.21	17.29	10.82	84.81−96.18	172.57−176.73	0.037	0.086	36e
XIII[a]	UKIPEJ	$Cu^{II}Mn^{II}$	−30	100.48	26.55	8.53	82.75−92.95	169.43−171.08	0.151	0.013	37a
XIV[a]	HETZIQ	$Cu^{II}Mn^{II}$	−19.5	99.22, 99.79	13.11, 13.85	15.72, 16.09	85.80−94.64, 84.02−95.38	170.32−177.13, 176.15−177.14	0.056, 0.054	0.104, 0.009	37b
XV[a]	YADNIB	$Cu^{II}Mn^{II}$-based polymer	−8.35	96.84	13.1	24.43	83.78−94.49	168.25	0.196	0.000	37c
XVI[a]	WAT-GON	$Cu^{II}Mn^{II}$	−13.5	96.20	14.31	23.54	84.22−94.95	164.98−171.08	0.201	0.051	37d
XVII[c]	FAEPCU	$Cu^{II}Mn^{II}$	−13.2	95.7	13.34	26.05	84.35−94.77	173.93−178.59	0.050	0.032	37e
XVIII[a,c]	FANHUZ	$Mn^{II}Cu^{II}_3$ star	−20.25, −20.25, −6.35	99.50, 99.93, 96.85	29.88, 35.65, 26.48	20.54, 15.69, 18.09	82.49−99.55, 82.97−99.10, 81.85−98.45	163.81−170.54, 159.91−170.88, 164.27−168.72	0.072, 0.131, 0.025	0.155, 0.186, 0.179	19b
1[d]		$Mn^{II}Cu^{II}_3$ star	1.02	100.15, 99.53	21.67, 20.13	4.62, 0.00	86.15−99.9, 86.58−100.6	143.45−148.72, 145.38	0.043, 0.000	0.544, 0.554	this work

[a]Square-pyramidal Cu^{II}. [b]Octahedral Cu^{II}. [c]Square-planar Cu^{II}. [d]Intermediate between square planar and tetrahedral. [e]Average value. [f]φ is the out-of-plane shift of the phenyl groups.

dx.doi.org/10.1021/ic501900d | Inorg. Chem. 2015, 54, 117−131

Table 5. Magnetic Exchange Integral and Some Relevant Structural Parameters of All Systems Where Copper(II) and Nickel(II) Are Bridged Solely by the Bis(μ_2-phenoxo) Moiety

							peripheral copper(II)				
compd no.	CSD code	compd type	J (cm^{-1})	Cu−O−Ni (a, deg)[d]	φ (deg)[d,e]	Cu−O−Ni−O (τ, deg)[d]	cis angle range (deg)	trans angle range (deg)	d_{Cu}(Å)	d_{NO} (Å)[d]	ref
XIX[a]	KAJFEG	$Fe^{III}Cu^{II}Ni^{II}$	−130	101.21	22.28	3.65	80.15−99.74	164.65−169.89	0.125	0.073	29
XX[a]	GIWYEQ	$Co^{III}Cu^{II}Ni^{II}$	−118.6	101.62	6.50	2.11	79.94−99.95	159.83−169.67	0.125	0.169	29
XXI[a]	KAHVAQ	$(Cu^{II}Ni^{II})_2$	−115	101.19	6.12	4.14	80.59−97.28	166.03−171.60	0.115	0.069	29
XXII[a]	LINWIO	$Cu^{II}Ni^{II}$	−47	101.58	6.60	17.88	76.70−99.47	160.82−161.54	0.254	0.015	29
XXIII[b]	IXAZUC	$Cu^{II}Ni^{II}Cu^{II}$	−50.6	101.12, 101.33	9.86, 9.04	2.92, 5.52	83.80−95.45, 85.08−94.81	176.19−178.52, 172.80−175.63	0.020, 0.024	0.040, 0.095	29
XXIV[a]	UKIPOT	$Cu^{II}Ni^{II}$	−67	100.88	24.91	6.97	81.77−94.20	169.50−171.30	0.146	0.010	29
XXV[a]	ZOJFEJ	$Cu^{II}Ni^{II}$	−90	99.86	12.60	6.27	83.85−97.04	173.14−177.31	0.076	0.035	30
XXVI[b]	BIHZEX	$Cu^{II}Ni^{II}$	−71	98.83	6.08	0.28	84.32−94.17	178.00−178.34	0.014	0.002	30
XXVII[a]	UDUWEV	$Cu^{II}Ni^{II}$	−12	94.54	38.01	15.78	85.57−95.35	162.48−178.92	0.146	0.139	30
XXVIII[b]	DEWPAW	$Cu^{II}Ni^{II}$	−11.8	93.17	13.55	27.49	83.93−95.62	177.41−177.51	0.008	0.035	30
2[c]		$Ni^{II}Cu^{II}_3$ star	−3.53	99.12	19.16	0.00	85.13−100.6	146.43	0.000	0.533	this work

[a]Square-pyramidal Cu^{II}. [b]Square-planar Cu^{II}. [c]Intermediate between square planar and tetrahedral. [d]Average value. [e]φ is the out-of-plane shift of the phenyl groups.

bis(μ_2-phenoxo) route has been determined in all of these complexes. Similar to the $Cu^{II}Mn^{II}$ cases, the roles of the phenoxo bond and metal···metal distances are unclear in the $Cu^{II}Ni^{II}$ systems also. In the previous 10 compounds, the range of the phenoxo bridge angle is 93.17−101.88° and the range of the J values is between −11.8 and −130 cm^{-1}. Although fluctuations are there in some cases and no straightforward correlation can be obtained (Figure S12 in the SI), interaction becomes generally more antiferromagnetic as the phenoxo bridge angle increases. On the other hand, the roles of τ and φ are not clear (Figures S13 and S14 in the SI).

Interestingly, compound **2** in the present investigation exhibits the smallest antiferromagnetic interaction (J = −3.53 cm^{-1}) between copper(II) and nickel(II) through the bis(μ_2-phenoxo) pathway, although the interaction should have been much more antiferromagetic in terms of the phenoxo bridge angle (99.12°). The situation is similar for **1** and **2**: antiferromagnetic interaction decreases for both, and in the case of **1**, this decrease is more prominent, giving rise to ferromagnetic interaction. The reason is also probably the same for the two compounds, i.e., huge distortion of the peripheral copper(II) geometry: the weight of the square-planar geometry is 52.8% in **2**, while it is 89.6−93.9%, or the values of the τ parameter are 0.01−0.274 in the previous 10 systems;[33,38] the trans angle in **2** is 146.43°, while they are 159.83−178.92° in the others; $d_{N/O}$ in **2** is 0.533 Å, while it is 0.002−0.169 Å in the others (Table 5).

As already mentioned, it is rather complicated to rationalize the extent of the magnetic exchange integral in the $Cu^{II}Cu^{II}_3$ compound **3** in light of the established magnetostructural correlations. However, because the phenoxo bridge angles in the equatorial−equatorial routes are 108.05 and 98.33°, the interaction in this compound also should have been stronger than −35.5 cm^{-1}. The reason for reduced antiferromagnetic interaction here also is most probably the enormous distortion of the peripheral copper(II) environment (trans angles, 142.63−150.55°; $d_{N/O}$, 0.53 Å).

The magnetic data for the $Zn^{II}Cu^{II}_3$ compound **4** were very satisfactorily simulated considering an intramolecular interaction of the copper(II) ions via the diamagnetic zinc ion with J = −1.4 cm^{-1}. This value is significantly larger than the one reported elsewhere for the interaction of manganese ions via the diamagnetic ions Cd^{2+}, Y^{3+}, Lu^{3+}, and Sr^{2+} ranging from −0.002 to −0.005 cm^{-1} but is much smaller than the −17.5 cm^{-1} reported for the interaction between copper(II) ions mediated by zinc(II) ions in the tetrahedral coordination geometry.[41] However, for compound **4**, the observed copper(II) exchange interaction of −1.4 cm^{-1} is very close to the estimated −1.6 cm^{-1} by Kahn and co-workers for an oxamido-bridged trinuclear $Cu^{II}Zn^{II}Cu^{II}$ complex.[42]

Theoretical Studies. DFT calculations have been carried out for the dicationic parts of the three stars $Mn^{II}Cu^{II}_3$ (**1**), $Ni^{II}Cu^{II}_3$ (**2**), and $Cu^{II}Cu^{II}_3$ (**3**). Unconstrained geometry optimizations were carried out for all three compounds, starting from either an isosceles or equilateral arrangement of the peripheral copper(II) centers. Only for compound **2** was a stable equilateral isomer found. This isomer was computed to be 2 kJ mol^{-1} higher in energy than the isosceles isomer, which, given the limits of accuracy of the present approach, does not exclude that this isomer is yet the more stable one in the experiment. The experimental and DFT-computed structural parameters are compared in Table S5 in the SI, revealing that calculations reproduce the experimental structures satisfactorily.

dx.doi.org/10.1021/ic501900d | Inorg. Chem. 2015, 54, 117−131

Table 6. Comparative DFT-Computed and Experimental Values of Magnetic Parameters along with Delocalization of Magnetic Orbitals of 1−3 (J Values in cm^{-1})

	$Mn^{II}Cu^{II}_3$ (1)		$Ni^{II}Cu^{II}_3$ (2)			$Cu^{II}Cu^{II}_3$ (3)	
	DFT (isosceles)	expt	DFT (isosceles)	DFT (equilateral)	expt	DFT (isosceles)	expt
			J				
J(M···Cu1)[a]	2.6	1.02	2.3	5.0	−3.53	−3.2	−35.5
J(M···Cu1A)[a]	2.6	1.02	2.3	5.0	−3.53	−3.2	−35.5
J(M···Cu2)[a]	1.0	1.02	−10.7	5.0	−3.53	−34.1	−35.5
J(Cu···Cu)	−0.8	−0.3	−1.4	−1.2	0.1	−1.8	0.6
J(Cu···Cu)	−0.6	−0.3	−0.7	−1.2	0.1	−3.3	0.6
			Delocalization[b]				
NLO-1	8		13	13		25	
NLO-2	8		13	13			
NLO-3	2						
NLO-4	2						
NLO-5	2						

[a]For the $Ni^{II}Cu^{II}_3$ (2) compound, Cu1A and Cu2 are Cu1B and Cu1C, respectively. For the $Cu^{II}Cu^{II}_3$ (3) compound, M is Cu3. [b]Percent delocalization of magnetic orbitals (NLOs) of the central ion.

Two different M···Cu interactions and two different peripheral Cu···Cu interactions were considered for the isosceles cases in compounds **1**−**3**, whereas one type of the each of the M···Cu and Cu···Cu interactions were considered for the equilateral case in compound **2**. The computed J values are listed in Tables 6 and S5 in the SI. For all three compounds, the calculated peripheral Cu···Cu J values are very small, lying in the overall range from −0.6 to −3.3 cm^{-1}. For compound **1**, all three computed Mn···Cu interactions are weakly ferromagnetic: J(M···Cu1)/J(M···Cu1A) = 2.6 cm^{-1} and J(M···Cu2) = 1.0 cm^{-1}. Thus, the DFT-computed exchange integrals are matched well with the experimental J values (J(M···Cu1)/J(M···Cu1A)/J(M···Cu2) = 1.02 cm^{-1}) in this case. For the isosceles $Ni^{II}Cu^{II}_3$, two computed J values are weakly ferromagnetic, 2.3/2.3 cm^{-1}, while the third is weakly antiferromagnetic, −10.7 cm^{-1}. On the other hand, the computed J values for the equilateral $Ni^{II}Cu^{II}_3$ are ferromagnetic, 5.0/5.0/5.0 cm^{-1}. Thus, although the experimental J values are weakly antiferromagnetic, −3.53/−3.53/−3.53 cm^{-1}, and the computed J values are either weakly ferromagnetic or weakly antiferromagnetic and weakly ferromagnetic, the qualitative matching is nice because both the experimental and computed results show reduced antiferromagnetic interaction in comparison to what one can expect from the established correlations such as Ni−phenoxo−Cu bridge angles. For the $Cu^{II}Cu^{II}_3$ compound **3**, the computed J(Cu3···Cu1)/J(Cu3···Cu1A) values, −3.2 cm^{-1}, are much less antiferromagnetic than the computed J(Cu3···Cu2) value, −34.1 cm^{-1}. As already discussed, such a difference in the two types of pathways is not unexpected. However, experimental data could not be simulated with even a slight difference in the J values (experimental J = −35.5/−35.5/−35.5 cm^{-1}). Here again, both the experimental and computed results show reduced antiferromagnetic interaction in comparison to what one can expect from the established correlations such as Cu−phenoxo−Cu bridge angles.

Magnetic orbitals (NLOs) of the central ion in **1**−**3** are shown in Figure 10, and their percentage delocalization are listed in Tables 6 and S5 in the SI. The order of the extent of delocalization of the magnetic orbitals is Mn^{II} in **1** (8, 8, 2, 2, and 2% for the five NLOs) < Ni^{II} in **2** (13 and 13% for the two NLOs for both the isosceles and equilateral cases) < Cu^{II} in **3** (25% for the single NLO). Small values (2−25%) of delocalization of magnetic orbitals clearly indicate that the title compounds should be weakly antiferromagnetic or ferromagnetic, which actually occurred. Again, the order of delocalization indicates that the order of antiferromagentic interaction should be **3** > **2** > **1**, which actually occurred, as is evidenced from both the experimental and DFT-computed J values; in the case of **1**, the interaction becomes ferromagnetic.

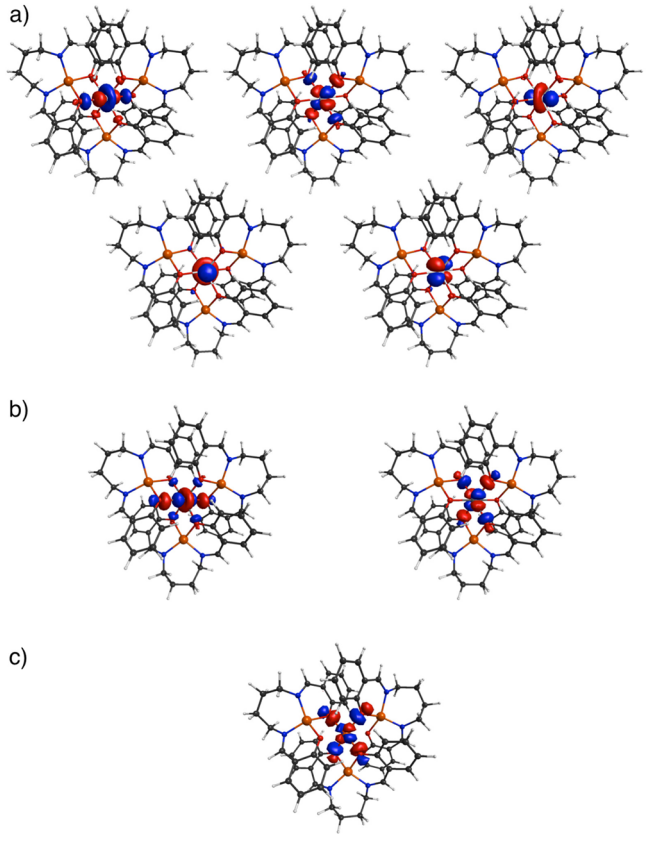

Figure 10. NLOs of (a) the $Mn^{II}Cu^{II}_3$ compound **1**, (b) the $Ni^{II}Cu^{II}_3$ compound **2**, and (c) the $Cu^{II}Cu^{II}_3$ compound **3**.

Spin densities of the high spin states of **1** (most ferromagnetic here) and **3** (most antiferromagnetic here) are shown in Figure 11. The spin density at the center is much more isotropic in **1** than in **3**, supporting ferromagnetic interaction in the former but antiferromagnetic in the latter.

dx.doi.org/10.1021/ic501900d | Inorg. Chem. 2015, 54, 117−131

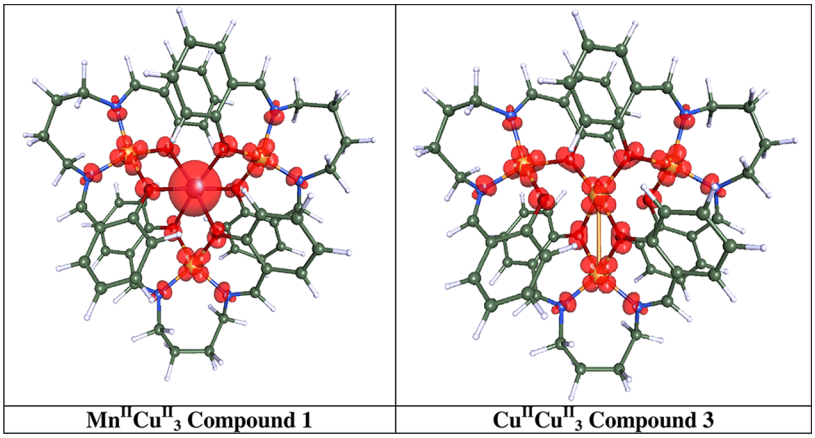

Figure 11. Spin density of the Mn^{II}Cu$^{II}_3$ compound **1** and Cu^{II}Cu$^{II}_3$ compound **3**.

Some test calculations show that other hybrid functionals like B3LYP give similar results, while GGAs like PBE give too much antiferromagnetic results, in accordance with the literature.[43]

CONCLUSIONS

A M^{II}Cu$^{II}_3$ star (M = Cd) has been previously reported by us from the single-compartment Schiff base ligand *N*,*N*′-bis(salicylidene)-1,4-butanediamine.[18a] Four more M^{II}Cu$^{II}_3$ stars [M = Mn (**1**), Ni (**2**), Cu (**3**), Zn (**4**)] are described in this report. Such a series of stars from the same ligand system is unprecedented. Clearly, *N*,*N*′-bis(salicylidene)-1,4-butanediamine is a potential ligand to stabilize tetrametallic M^{II}Cu$^{II}_3$ stars. It may also be mentioned that compound **1** is only the second example of a Mn^{II}Cu$^{II}_3$ star, while compounds **2**−**4** are the sole examples of a Ni^{II}Cu$^{II}_3$/Cu^{II}Cu$^{II}_3$/Zn^{II}Cu$^{II}_3$ star. Although there are many homo- and heterometallic compounds derived from single/double-compartmental ligands, only a few (<10 including **1**−**4**) are star compounds.

The Cu^{II}Cu$^{II}_3$ (**3**) and Ni^{II}Cu$^{II}_3$ (**2**) compounds exhibit antiferromagnetic interaction with *J* values respectively of −35.5 and −3.53 cm^{-1}, while the interaction between copper(II) and manganese(II) in the Mn^{II}Cu$^{II}_3$ (**1**) compound is ferromagnetic with *J* = 1.02 cm^{-1}. On the basis of the usual governing parameters such as the phenoxo bridge angle, metal−O−metal−O torsion angle, and out-of-plane shift of the phenyl groups, the interaction in all of **1**−**3** should have been more antiferromagnetic. Because the structural parameters around the manganese(II) or nickel(II) coordination environment cannot shed light on the magnetic properties, it seems that the large distortion in the environment of peripheral copper(II) is the origin of unusually reduced antiferromagnetic (in **2**) or ferromagnetic (in **1**) interaction. The reason for the reduced antiferromagnetic interaction in the Cu^{II}Cu$^{II}_3$ (**3**) compound is therefore probably the same.

DFT-computed *J* values are matched well either quantitatively (for **1**) or qualitatively (for **2** and **3**) with the experimental values. Spin densities correspond well with the ferromagnetic interaction in **1** and antiferromagnetic interaction in **3**. DFT-computed magnetic orbitals (NBOs) clearly indicate that interactions in **1**−**3** should be either ferromagnetic or reduced antiferromagnetic, which is actually observed experimentally.

ASSOCIATED CONTENT

Supporting Information

Crystallographic data of **1**−**4** in CIF format, Tables S1−S5, and Figures S1−S14. This material is available free of charge via the Internet at http://pubs.acs.org.

AUTHOR INFORMATION

Corresponding Authors

*E-mail: rentschl@uni-mainz.de.
*E-mail: sm_cu_chem@yahoo.co.in.

Notes

The authors declare no competing financial interest.

ACKNOWLEDGMENTS

Financial support, including a postdoctoral fellowship (to A.J.), for this work has been received from the Department of Science and Technology, the Government of India (Project SR/S1/IC-42/2011 to Sa.M.). Su.M. acknowledges the Council for Scientific and Industrial Research for providing a fellowship. Sh.M. acknowledges the DST for providing a DST-INSPIRE fellowship. Crystallography was performed at the DST-FIST, an India-funded Single Crystal Diffractometer Facility at the Department of Chemistry, University of Calcutta.

REFERENCES

(1) (a) Guha, B. *Proc. R. Soc. London* **1951**, *A206*, 353. (b) Bleaney, B.; Bowers, K. D. *Proc. R. Soc. London* **1952**, *A214*, 451.

(2) (a) Kahn, O. *Molecular Magnetism*; VCH Publications: New York, 1993. (b) *Magneto-Structural Correlations in Exchange Coupled Systems*; Willet, R. D., Gatteschi, D., Kahn, O., Eds.; Reidel: Dordrecht, The Netherlands, 1985. (c) Ribas, J.; Escuer, A.; Monfort, M.; Vicente, R.; Cortés, R.; Lezama, L.; Rojo, T. *Coord. Chem. Rev.* **1999**, *193*−*195*, 1027−1068.

(3) (a) Langley, S. K.; Chilton, N. F.; Moubaraki, B.; Murray, K. S. *Inorg. Chem.* **2013**, *52*, 7183−7192. (b) Langley, S. K.; Chilton, N. F.; Moubaraki, B.; Murray, K. S. *Inorg. Chem.* **2013**, *52*, 8280−8280. (c) Chilton, N. F.; Deacon, G. B.; Gazukin, O.; Junk, P. C.; Kersting, B.; Langley, S. K.; Moubaraki, B.; Murray, K. S.; Schleife, F.; Shome, M.; Turner, D. R.; Walker, J. A. *Inorg. Chem.* **2014**, *53*, 2528−2534.

(4) (a) Tidmarsh, I. S.; Batchelor, L. J.; Scales, E.; Laye, R. H.; Sorace, L.; Caneschi, A.; Schnack, J.; McInnes, E. J. L. *Dalton Trans.* **2009**, 9402−9409. (b) Alborés, P.; Rentschler, E. *Inorg. Chem.* **2008**, *47*, 7960−7962. (c) Cariati, E.; Ugo, R.; Santoro, G.; Tordin, E.; Sorace, L.; Caneschi, A.; Sironi, A.; Macchi, P.; Casati, N. *Inorg. Chem.* **2010**, *49*, 10894−10901.

(5) (a) Darmon, J. M.; Chantal, S.; Stieber, E.; Sylvester, K. T.; Fernández, I.; Lobkovsky, E.; Semproni, S. P.; Bill, E.; Wieghardt, K.; DeBeer, S.; Chirik, P. J. *J. Am. Chem. Soc.* **2012**, *134*, 17125−17137. (b) Bowman, A. C.; Milsmann, C.; Bill, E.; Lobkovsky, E.; Weyhermüller, T.; Wieghardt, K.; Chirik, P. J. *Inorg. Chem.* **2010**, *49*, 6110−6123. (c) Arumugam, K.; Shaw, M. C.; Mague, J. T.; Bill, E.; Sproules, S.; Donahue, J. P. *Inorg. Chem.* **2011**, *50*, 2995−3002.

(6) (a) Alborés, P.; Rentschler, E. *Inorg. Chem.* **2008**, *47*, 7960−7962. (b) Alborés, P.; Slep, L. D.; Baraldo, L. M.; Baggio, R.; Garland, M. T.; Rentschler, E. *Inorg. Chem.* **2006**, *45*, 2361−2363.
(7) (a) Sessoli, R.; Gatteschi, D.; Caneschi, A.; Novak, M. A. *Nature* **1993**, *365*, 141−143. (b) Aromí, G.; Brechin, E. K. *Struct. Bonding (Berlin)* **2006**, *122*, 1−67. (c) Murrie, M. *Chem. Soc. Rev.* **2010**, *39*, 1986−1995. (d) Mukherjee, S.; Abboud, K. A.; Wernsdorfer, W.; Christou, G. *Inorg. Chem.* **2013**, *52*, 873−884. (e) Woodruff, D. N.; Winpenny, R. E. P.; Layfield, R. A. *Chem. Rev.* **2013**, *113*, 5110−5148. (f) Rinehart, J. D.; Long, J. R. *Chem. Sci.* **2011**, *2*, 2078−2085. (g) Sorace, L.; Benelli, C.; Gatteschi, D. *Chem. Soc. Rev.* **2011**, *40*, 3092−3104. (h) Sessoli, R.; Powell, A. K. *Coord. Chem. Rev.* **2009**, *253*, 2328−2341.
(8) (a) Botana, L.; Ruiz, J.; Seco, J. M.; Mota, A. J.; Rodríguez-Diéguez, A.; Sillanpää, R.; Colacio, E. *Dalton Trans.* **2011**, *40*, 12462−12471. (b) Wichmann, O.; Sopo, H.; Colacio, E.; Mota, A. J.; Sillanpää, R. *Eur. J. Inorg. Chem.* **2009**, 4877−4886. (c) Laborda, S.; Clérac, R.; Anson, C. E.; Powell, A. K. *Inorg. Chem.* **2004**, *43*, 5931−5943. (d) Thompson, L. K.; Mandal, S. K.; Tandon, S. S.; Bridson, J. N.; Park, M. K. *Inorg. Chem.* **1996**, *35*, 3117−3125. (e) Crawford, V. M.; Richardson, H. W.; Wasson, J. R.; Hodgson, D. J.; Hatfield, W. E. *Inorg. Chem.* **1976**, *15*, 2107−2110. (f) Merz, L.; Haase, W. *J. Chem. Soc., Dalton Trans.* **1980**, 875−879.
(9) (a) Hazra, S.; Bhattacharya, S.; Singh, M. K.; Carrella, L.; Rentschler, E.; Weyhermüller, T.; Rajaraman, G.; Mohanta, S. *Inorg. Chem.* **2013**, *52*, 12881−12892. (b) Sasmal, S.; Hazra, S.; Kundu, P.; Dutta, S.; Rajaraman, G.; Sañudo, E. C.; Mohanta, S. *Inorg. Chem.* **2011**, *50*, 7257−7267. (c) Sasmal, S.; Hazra, S.; Kundu, P.; Majumder, S.; Aliaga-Alcalde, N.; Ruiz, E.; Mohanta, S. *Inorg. Chem.* **2010**, *49*, 9517−9526.
(10) (a) Nanda, K. K.; Thompson, L. K.; Bridson, J. N.; Nag, K. *Chem. Commun.* **1994**, 1337−1338. (b) Mohanta, S.; Nanda, K. K.; Thompson, L. K.; Flörke, U.; Nag, K. *Inorg. Chem.* **1998**, *37*, 1465−1472. (c) Palacios, M. A.; Mota, A. J.; Perea-Buceta, J. E.; White, F. J.; Brechin, E. K.; Colacio, E. *Inorg. Chem.* **2010**, *49*, 10156−10165. (d) Costes, J.-P.; Dahan, F.; Dupuis, A. *Inorg. Chem.* **2000**, *39*, 165−168.
(11) (a) Kurtz, D. M., Jr. *Chem. Rev.* **1990**, *90*, 585−606. (b) Weihe, H.; Güdel, H. U. *J. Am. Chem. Soc.* **1997**, *119*, 6539−6543. (c) Gall, F. L.; Biani, F. F. d.; Caneschi, A.; Cinelli, P.; Cornia, A.; Fabretti, A. C.; Gatteschi, D. *Inorg. Chim. Acta* **1997**, *262*, 123−132. (d) Hänninen, M. M.; Colacio, E.; Mota, A. J.; Sillanpää, R. *Eur. J. Inorg. Chem.* **2011**, 1990−1996.
(12) Law, N. A.; Kampf, J. W.; Pecoraro, V. L. *Inorg. Chim. Acta* **2000**, *297*, 252−264.
(13) (a) Venegas-Yazigi, D.; Aravena, D.; Spodine, E.; Ruiz, E.; Alvarez, S. *Coord. Chem. Rev.* **2010**, *254*, 2086−2095. (b) Ruiz, E.; Graaf, C. d.; Alemany, P.; Alvarez, S. *J. Phys. Chem. A* **2002**, *106*, 4938−4941. (c) Ruiz, E.; Alemany, P.; Alvarez, S.; Cano, J. *J. Am. Chem. Soc.* **1997**, *119*, 1297−1303. (d) Rodríguez-Fortea, A.; Alemany, P.; Alvarez, S.; Ruiz, E. *Inorg. Chem.* **2002**, *41*, 3769−3778. (e) Ruiz, E.; Cano, J.; Alvarez, S.; Alemany, P. *J. Am. Chem. Soc.* **1998**, *120*, 11122−11129. (f) Triki, S.; Gómez-García, C. J.; Ruiz, E.; Sala-Pala, J. *Inorg. Chem.* **2005**, *44*, 5501−5508.
(14) (a) Rajaraman, G.; Totti, F.; Bencini, A.; Caneschi, A.; Sessoli, R.; Gatteschi, D. *Dalton Trans.* **2009**, 3153−3161. (b) Singh, S. K.; Tibrewal, N. K.; Rajaraman, G. *Dalton Trans.* **2011**, *40*, 10897−10906. (c) Rajeshkumar, T.; Rajaraman, G. *Chem. Commun.* **2012**, *48*, 7856−7858.
(15) *The Cambridge Structural Database (CSD)*, version 5.34; The Cambridge Crystallographic Data Center: Cambridge, U.K., 2012.
(16) (a) Hall, D.; Waters, T. N. *J. Chem. Soc.* **1960**, 2644−2648. (b) Scheringer, C.; Hinkler, K.; Stackelberg, M. V. *Z. Anorg. Allg. Chem.* **1960**, *306*, 35−38.
(17) (a) Jana, A.; Mohanta, S. *CrystEngComm* **2014**, *16*, 5494 and references cited therein. (c) Andruh, M.; Branzea, D. G.; Gheorghe, R.; Madalan, A. M. *CrystEngComm* **2009**, *11*, 2571−2584 and references cited therein. (c) Winpenny, R. E. P. *Chem. Soc. Rev.* **1998**, *27*, 447−452.
(18) (a) Mondal, S.; Mandal, S.; Jana, A.; Mohanta, S. *Inorg. Chim. Acta* **2014**, *415*, 138−145 and references cited therein. (b) Bhattacharya, S.; Jana, A.; Fleck, M.; Mohanta, S. *Inorg. Chim. Acta* **2013**, *405*, 196−202. (c) Biswas, A.; Mandal, L.; Mondal, S.; Lucas, C. R.; Mohanta, S. *CrystEngComm* **2013**, *15*, 5888−5897. (d) Nayak, M.; Koner, R.; Lin, H.-H.; Flölrke, U.; Wei, H.-H.; Mohanta, S. *Inorg. Chem.* **2006**, *45*, 10764−10773. (e) Biswas, A.; Ghosh, M.; Lemoine, P.; Sarkar, S.; Hazra, S.; Mohanta, S. *Eur. J. Inorg. Chem.* **2010**, 3125−3134. (f) Nayak, M.; Hazra, S.; Lemoine, P.; Koner, R.; Lucas, C. R.; Mohanta, S. *Polyhedron* **2008**, *27*, 1201−1231. (g) Nayak, M.; Koner, R.; Lin, H.-H.; Flörke, U.; Wei, H.-H.; Mohanta, S. *Inorg. Chem.* **2006**, *45*, 10764−10773. (h) Koner, R.; Lin, H.-H.; Wei, H.-H.; Mohanta, S. *Inorg. Chem.* **2005**, *44*, 3524−3536. (i) Koner, R.; Lee, G.-H.; Wang, Y.; Wei, H.-H.; Mohanta, S. *Eur. J. Inorg. Chem.* **2005**, 1500−1505.
(19) (a) Gulino, A.; Fragala, I. L.; Lupo, F.; Malandrino, G.; Motta, A.; Colombo, A.; Dragonetti, C.; Righetto, S.; Roberto, D.; Ugo, R.; Demartin, F.; Ledoux-Rak, I.; Singh, A. *Inorg. Chem.* **2013**, *52*, 7550−7556. (b) Biswas, S.; Naiya, S.; Gomez-Garcia, C. J.; Ghosh, A. *Dalton Trans.* **2012**, *41*, 462−673. (c) Biswas, S.; Naiya, S.; Drew, M. G. B.; Estarellas, C.; Frontera, A.; Ghosh, A. *Inorg. Chim. Acta* **2011**, *366*, 219−226. (d) Biswas, S.; Ghosh, A. *Polyhedron* **2011**, *30*, 676−681. (e) Pointillart, F.; Bernot, K. *Eur. J. Inorg. Chem.* **2010**, 952−964. (f) Yamaguchi, T.; Costes, J.-P.; Kishima, Y.; Kojima, M.; Sunatsuki, Y.; Bréfuel, N.; Tuchagues, J.-P.; Vendier, L.; Wernsdorfer, W. *Inorg. Chem.* **2010**, *49*, 9125−9135. (g) Lü, Z.; Yuan, M.; Pan, F.; Gao, S.; Zhang, D.; Zhu, D. *Inorg. Chem.* **2006**, *45*, 3538−3548. (h) Feng, Y.; Wanga, C.; Zhao, Y.; Li, J.; Liao, D.; Yan, S.; Wang, Q. *Inorg. Chim. Acta* **2009**, *362*, 3563−3568. (i) Wei, T.; Zhao, S.; Bi, W.; Lü, X.; Hui, Y.; Song, J.; Wong, W.-K.; Jones, R. A. *Inorg. Chem. Commun.* **2009**, *12*, 1216−1219.
(20) (a) Rajendiran, T. M.; Kannappan, R.; Mahalakshmi, R.; Venkatesan, R.; Rao, P. S.; Govindaswamy, L.; Velmurugan, D. *Transition Met. Chem.* **2003**, *28*, 644−649. (b) Yang, X.; Lam, D.; Chan, C.; Stanley, J. M.; Jones, R. A.; Holliday, B. J.; Wong, W.-K. *Dalton Trans.* **2011**, *40*, 9795−9801. (c) Clarke, B.; Cunningham, D.; Gallagher, J. F.; Higgins, T.; McArdle, P.; McGinley, J.; Cholchuin, M. N.; Sheerin, D. *J. Chem. Soc., Dalton Trans.* **1994**, 2473−2482. (d) You, Z.-L.; Lu, Y.; Zhang, N.; Ding, B.-W.; Sun, H.; Hou, P.; Wang, C. *Polyhedron* **2011**, *30*, 2186−2194. (e) Yildirim, L. T.; Kurtaran, R.; Namli, H.; Azaz, A. D.; Atakol, O. *Polyhedron* **2007**, *26*, 4187−4194.
(21) (a) Salmon, L.; Thuery, P.; Riviere, E.; Ephritikhine, M. *Inorg. Chem.* **2006**, *45*, 83−93. (b) Reglinski, J.; Morris, S.; Stevenson, D. E. *Polyhedron* **2002**, *21*, 2175−2182. (c) Sanmartin, J.; Bermejo, M. R.; Garcia-Deibe, A. M.; Llamas-Saiz, A. L. *Chem. Commun.* **2000**, 795−796. (d) Reglinski, J.; Morris, S.; Stevenson, D. E. *Polyhedron* **2002**, *21*, 2167−2174. (e) You, Z.-L.; Zhu, H.-L.; Liu, W.-S. *Z. Anorg. Allg. Chem.* **2004**, *630*, 1617−1622.
(22) (a) Thewalt, U.; Müller, S. *Chem. Ber.* **1988**, *121*, 2111. (b) Müller, S.; Thewalt, U. *Z. Naturforsch. B: Chem. Sci.* **1989**, *44*, 257. (c) Hodgson, D. J.; Michelsen, K.; Pedersen, E.; Towle, D. K. *J. Chem. Soc., Chem. Commun.* **1988**, 426−428. (d) Tancini, E.; Rodriguez-Douton, M. J.; Sorace, L.; Barra, A.-L.; Sessoli, R.; Cornia, A. *Chem.—Eur. J.* **2010**, *16*, 10482−10493. (e) Mannini, M.; Tancini, E.; Sorace, L.; Sainctavit, P.; Arrio, M.-A.; Qian, Y.; Otero, E.; Chiappe, D.; Margheriti, L.; Cezar, J. C.; Sessoli, R.; Cornia, A. *Inorg. Chem.* **2011**, *50*, 2911−2917. (f) Totaro, P.; Westrup, K. C. M.; Boulon, M.-E.; Nunes, G. G.; Back, D. F.; Barison, A.; Ciattini, S.; Mannini, M.; Sorace, L.; Soares, J. F.; Cornia, A.; Sessoli, R. *Dalton Trans.* **2013**, *42*, 4416−4426. (g) Feltham, H. L. C.; Clérac, R.; Powell, A. K.; Brooker, S. *Inorg. Chem.* **2011**, *50*, 4232−4234. (h) Feltham, H. L. C.; Clérac, R.; Ungur, L.; Chibotaru, L. F.; Powell, A. K.; Brooker, S. *Inorg. Chem.* **2013**, *52*, 3236−3240.
(23) (a) *APEX-II*, *SAINT-Plus*, and *TWINABS*; Bruker-Nonius AXS Inc.: Madison, WI, 2004. (b) Sheldrick, G. M. *SAINT*, version 6.02; *SADABS*, version 2.03; Bruker AXS Inc.: Madison, WI, 2002. (c) *SHELXTL*, version 6.10; Bruker AXS Inc.: Madison, WI, 2002. (d) Sheldrick, G. M. *SHELXL-97, Crystal Structure Refinement Program*; University of Göttingen: Göttingen, Germany, 1997.

(e) Spek, A. L. *PLATON, A Multipurpose Crystallographic Tool*; Utrecht University: Utrecht, The Netherlands, 2008.
(24) *TURBOMOLE V6.5 2013, a development of University of Karlsruhe and Forschungszentrum Karlsruhe GmbH, 1989−2007*, TURBOMOLE GmbH since 2007; available from http://www.turbomole.com.
(25) (a) Perdew, J. P.; Burke, K.; Ernzerhof, M. *Phys. Rev. Lett.* **1996**, *77*, 3865. (b) Ernzerhof, M.; Scuseria, G. E. *J. Chem. Phys.* **1999**, *110*, 5029.
(26) Sierka, M.; Hogekamp, A.; Ahlrichs, R. *J. Chem. Phys.* **2003**, *118*, 9136.
(27) Weigend, F.; Ahlrichs, R. *Phys. Chem. Chem. Phys.* **2005**, *7*, 3297.
(28) Weigend, F. *Phys. Phys. Chem. Chem. Phys.* **2006**, *8*, 1057.
(29) Grimme, S.; Antony, J.; Ehrlich, S.; Krieg, H. *J. Chem. Phys.* **2010**, *132*, 154104.
(30) Noodleman, L. J. *Chem. Phys.* **1981**, *74*, 5737.
(31) Pipek, J.; Mezey, P. G. *J. Chem. Phys.* **1989**, *90*, 4916.
(32) Bode, B. M.; Gordon, M. S. *J. Mol. Graphics Model.* **1998**, *16*, 133.
(33) (a) Pinsky, M.; Avnir, D. *Inorg. Chem.* **1998**, *37*, 5575−5582. (b) Casanova, D.; Cirera, J.; Llunell, M.; Alemany, P.; Avnir, D.; Alvarez, S. *J. Am. Chem. Soc.* **2004**, *126*, 1755−1763. (c) Cirera, J.; Ruiz, E.; Alvarez, S. *Chem.—Eur. J.* **2006**, *12*, 3162−3167.
(34) (a) Saalfrank, R. W.; Bernt, I.; Chowdhry, M. M.; Hampel, F.; Vaughan, G. B. M. *Chem.—Eur. J.* **2001**, *7*, 2765−2769. (b) Accorsi, S.; Barra, A.-L.; Caneschi, A.; Chastanet, G.; Cornia, A.; Fabretti, A. C.; Gatteschi, D.; Mortalò, C.; Olivieri, E.; Parenti, F.; Rosa, P.; Sessoli, R.; Sorace, L.; Wernsdorfer, W.; Zobbi, L. *J. Am. Chem. Soc.* **2006**, *128*, 4742−4755. (c) Barra, A. L.; Caneschi, A.; Cornia, A.; Fabrizi de Biani, F.; Gatteschi, D.; Sangregorio, C.; Sessoli, R.; Sorace, L. *J. Am. Chem. Soc.* **1999**, *121*, 5302−5310. (d) Gao, E.-Q.; Bai, S.-Q.; He, Z.; Yan, C.-H. *Inorg. Chem.* **2005**, *44*, 677−682. (e) Batchelor, L. J.; Sander, M.; Tuna, F.; Helliwell, F.; Moro, F.; Slageren, J. V.; Burzurí, E.; Montero, O.; Evangelisti, M.; Luis, F.; McInnes, E. J. L. *Dalton Trans.* **2011**, *40*, 5278−5284.
(35) Chilton, N. F.; Anderson, R. P.; Turner, L. D.; Soncini, A.; Murray, K. S. *J. Comput. Chem.* **2013**, *34*, 1164−1175.
(36) (a) Branzea, D. G.; Madalan, A. M.; Ciattini, S.; Avarvari, N.; Caneschi, A.; Andruh, M. *New J. Chem.* **2010**, *34*, 2479−2490. (b) Branzea, D. G.; Guerri, A.; Fabelo, O.; Ruiz-Pérez, C.; Chamoreau, L.-M.; Sangregorio, C.; Caneschi, A.; Andruh, M. *Cryst. Growth Des.* **2008**, *8*, 941−949. (c) Osa, S.; Sunatsuki, Y.; Yamamoto, Y.; Nakamura, M.; Shimamoto, T.; Matsumoto, N.; Re, N. *Inorg. Chem.* **2003**, *42*, 5507−5512. (d) Bo, L.; Hong, Z.; Zhi-Quan, P.; You, S.; Cheng-Gang, W.; Han-Ping, Z.; Jing-Dong, H.; Ru-An, C. *J. Coord. Chem.* **2006**, *59*, 1271−1280. (e) Ruiz, R.; Lloret, F.; Julve, M.; Faus, J. *Inorg. Chim. Acta* **1993**, *213*, 261−268.
(37) (a) Hori, A.; Mitsuka, Y.; Ohba, M.; Ōkawa, H. *Inorg. Chim. Acta* **2002**, *337*, 113−121. (b) Visinescu, D.; Sutter, J.-P.; Ruiz-Pérez, C.; Andruh, M. *Inorg. Chim. Acta* **2006**, *359*, 433−440. (c) Pascu, M.; Lloret, F.; Avarvari, N.; Julve, M.; Andruh, M. *Inorg. Chem.* **2004**, *43*, 5189−5191. (d) Ōkawa, H.; Nishio, J.; Ohba, M.; Tadokoro, M.; Matsumoto, N.; Koikawa, M.; Kida, S.; Fenton, D. E. *Inorg. Chem.* **1993**, *32*, 2949−2957. (e) O'connor, C. J.; Freyberg, D. P.; Sinn, E. *Inorg. Chem.* **1979**, *18*, 1077−1088.
(38) Hoskins, B. F.; Whillans, F. D. *Coord. Chem. Rev.* **1973**, *9*, 365−388.
(39) (a) Verani, C. N.; Rentschler, E.; Weyhermüller, T.; Bill, E.; Chaudhuri, P. *Dalton Trans.* **2000**, 251−258. (b) Verani, C. N.; Weyhermüller, T.; Rentschler, E.; Bill, E.; Chaudhuri, P. *Chem. Commun.* **1998**, 2475−2476. (c) Yonemura, M.; Ohba, M.; Takahashi, K.; Ōkawa, H.; Fenton, D. E. *Inorg. Chim. Acta* **1998**, *283*, 72−79. (d) Tao, R.-J.; Mei, C.-Z.; Zang, S.-Q.; Wang, Q.-L.; Niu, J.-Y.; Liao, D.-Z. *Inorg. Chim. Acta* **2004**, *357*, 1985−1990. (e) Hori, A.; Mitsuka, Y.; Ohba, M.; Ōkawa, H. *Inorg. Chim. Acta* **2002**, *337*, 113−121.
(40) (a) Aono, T.; Wada, H.; Aratake, Y.-I.; Matsumoto, N.; Ōkawa, H.; Matsuda, Y. *Dalton Trans.* **1996**, 25−29. (b) Morgenstern-Badarau, I.; Rerat, M.; Khan, O.; Jaud, J.; Galy, J. *Inorg. Chem.* **1982**, *21*, 3050−3059. (c) Yonemura, M.; Arimura, K.; Inoue, K.; Usuki, N.; Ohba, M.; Ōkawa, H. *Inorg. Chem.* **2002**, *41*, 582−589. (d) Journaux, Y.; Kahn, O.; Morgenstern-Badarau, I.; Galy, J.; Jaud, J.; Bencini, A.; Gatteschi, D. *J. Am. Chem. Soc.* **1985**, *107*, 6305−6312.
(41) (a) Ako, A. M.; Burger, B.; Lan, Y. H.; Mereacre, V.; Clerac, R.; Buth, G.; Gomez-Coca, S.; Ruiz, E.; Anson, C. E.; Powell, A. K. *Inorg. Chem.* **2013**, *52*, 5764−5774. (b) Buvaylo, E. A.; Kokozay, V. N.; Vassilyeva, O. Y.; Skelton, B. W.; Jezierska, J.; Brunel, L. C.; Ozarowski, A. *Chem. Commun.* **2005**, 4976−4978.
(42) Journaux, Y.; Sletten, J.; Kahn, O. *Inorg. Chem.* **1986**, *25*, 439−447.
(43) Cabrero, J.; Calzado, C. J.; Maynau, D.; Caballol, R.; Malrieu, J. P. *J. Phys. Chem. A* **2002**, *106*, 8146.